KEVIN S. McKELVEY
U.S. Forest Service
Redwood Sciences Laboratory
Arcata, California

KELLY K. BUSSE
U.S. Forest Service
Redwood Sciences Laboratory
Arcata, California

41

Twentieth-Century Fire Patterns on Forest Service Lands

ABSTRACT

Maps of twentieth-century fires on Forest Service lands were analyzed. Time trends showed no overall trend in acreage, but human-caused fires decreased and lightning fires increased. The increase in lightning fire was dominated by two recent years (1987 and 1990), but more subtle trends prior to 1987 indicated that lightning fires were following a trajectory separate from that of human-caused fires. Landscape-level analysis indicated a strong and stable elevation gradient in burn frequency, and this allowed the development of an accurate descriptive model. An analysis relating fire frequency to vegetation type showed that certain types of vegetation burn more than expected given their elevation, but that burning within these types followed the general trend, with higher-elevation types burning less frequently.

An analysis of reburn patterns showed that, given a particular risk zone, fire location is nearly random. Acreage that burned more than three times had a greater burn frequency than would be expected if the fires were random, but the total area with multiple burns was tiny. The location of multiple-burn sites indicated that they were associated with special features such as busy roads.

Fire correlations with general weather indices were weak, but more area burned in hot, dry years. Perhaps more importantly, all of the extreme fire years occurred when it was hot and dry. Short-term (1979–89) analyses of drought patterns indicated that drought decreased with increasing elevation, paralleling the decrease in fire frequency. Periods of drought were highly synchronized between weather stations, increasing the window during which extreme fire events could occur at all elevations.

The strong and stable elevation trends in fire frequency indicated that future risk could be inferred from twentieth-century fire patterns. The largely random location of fires within each risk zone indicated that a general zonal strategy for fire control would be most effective. The fire acreage patterns over time indicate that while suppression and possibly education can reduce human-caused fires, large lightning fires will continue to occur. Overall risk will vary with weather, but we can expect that large fires will occur during future droughts. If the weather in the twenty-first century is similar to weather in the twentieth century, we might reasonably expect 40% to 60% of the foothills zone to see fire at least once in the next 100 years.

INTRODUCTION

Determining the nature of fire patterns on the landscape is fundamental to both fire ecology and the assessment of fire risk. Critical questions include how often an area can be expected to burn, the size distribution of fires, the impacts of weather and changes in vegetation on fire patterns, and likely fire effects.

In 1994, maps of historical fires on U.S. Forest Service lands were collated to support the development of the California spotted owl environmental impact statement (CALOWL EIS) (USFS 1996). Mapped fires covered a period from 1900 to 1993, with reasonably complete coverage from 1908 to 1992. One forest, the Inyo, didn't report any fires prior to 1960 (Erman and Jones 1996). In all, 2,536 fires, ranging in size from 1 ha (2.5 acres) to more than 50,000 ha (123,500 acres), were individually mapped, digitized, and properly georeferenced. Small fires (less than 1 ha) were not mapped, and therefore these data represent a subset of all fires and only part of the acreage. However, the mapped fires are probably those that are most important biologically, financially, and socially. These are the fires that escaped initial containment and were, at least for a time, uncontrolled.

Sierra Nevada Ecosystem Project: Final report to Congress, vol. II, *Assessments and scientific basis for management options.* Davis: University of California, Centers for Water and Wildland Resources, 1996.

While these maps are not a complete set of all fires, they probably include most of the acreage burned (Strauss et al. 1989), and, because they were made available in digital format, they represent a remarkable and rich information source concerning the nature of fire in the twentieth-century Sierra Nevada.

Utilizing these maps, we have been able to address several important questions concerning fire. In this chapter, we first analyze the general patterns in acreage over time. We then examine the location and frequency of fire on the landscape, including reburn patterns, and lastly we explore the relationships between fire patterns and weather. Because of the large number of analyses associated with these topics, each is presented separately, with the major themes summarized at the end.

Because of data availability, the time period varied with each analysis. For analyses of general fire patterns, all mapped fires (1900–1993) were utilized. If yearly data were used, the time series was narrowed to 1908–92, the years in which coverage appeared to be reasonably complete. Representative weather data were not available prior to 1933, and the daily weather database we utilized extends only to 1989. Most of the analyses involving weather, therefore, extended from 1933–89. Lastly, because the number of reporting stations in the mountains has increased in recent years, analyses of weather changes with elevation utilized the years 1979–89.

EVALUATING ACREAGE BURNED OVER TIME

The number of mapped fires decreased with fire size, following a linear pattern when graphed on a log-log scale (figure 41.1). This pattern, which is similar to fire patterns developed for Southern California (Minnich 1983), means that there are many small fires and a few large fires. The fire acreage was quite variable from year to year and showed no time trend in yearly area burned (figure 41.2; $r^2 = 0.01$, $p = 0.33$). When viewed as a cumulative distribution, total acres burned appeared to increase in spurts in the 1920s, late 1950s, and late 1980s with slower, but rather constant, increases in between (figure 41.3).

While there are no significant trends in overall acreage burned, a number of weak, but significant, patterns were detected. The total number of fires between 1908 and 1992 decreased ($r^2 = 0.09$, $p = 0.005$), and the proportion of the total yearly acreage contributed by the largest fire increased ($r^2 = 0.11$, $p = 0.002$). Neither of these trends was very strong, and neither appears to be linear (figure 41.4). The divergence in fire size, for instance, was strongly influenced by three large fires that occurred since 1940 (figure 41.5). Due to their large size, these fires caused a significant shift in the acreage distribution (figure 41.6).

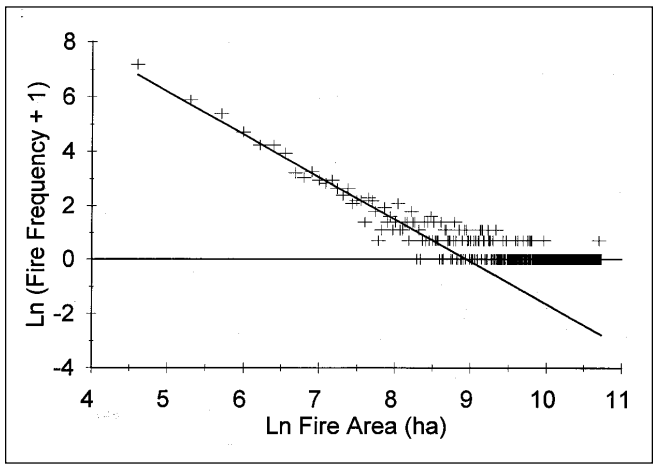

FIGURE 41.1

Number of fires as a function of size on U.S. Forest Service lands. All mapped fires (1900–1993) are included. Both axes are ln transformed.

The relative importance of people and lightning as ignition sources has also changed over time. Over the course of the twentieth century, human-caused fires dominated, both in numbers and in area. Of the 2,536 fires mapped by the Forest Service, 2,046 were caused by humans. This same pattern was reflected in the acreage statistics, with 1,164,439 ha (2,876,164 acres) attributable to human causes and 277,110 ha (684,462 acres) attributable to lightning. Although the number of human-caused fires decreased over time ($r^2 = 0.17$, $p < 0.001$), the dominance of humans as a fire source remained constant for most of the century.

In the late 1980s, however, this pattern changed radically (figure 41.7). In 1987 and 1990, lightning-caused fires domi-

FIGURE 41.2

Yearly area burned between 1908 and 1992. The years 1900–1907 and 1993 are excluded due to incomplete fire records.

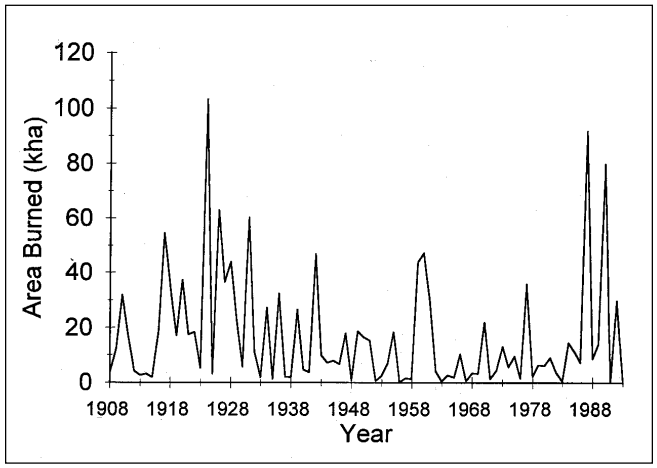

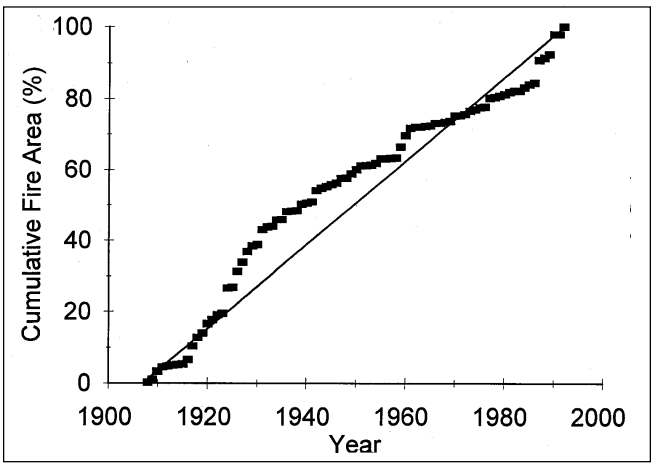

FIGURE 41.3

Cumulative fire area burned between 1908 and 1992. The line represents the rate of increase, assuming a constant area burned per year.

nated the fire acreage. These lightning fires were also unusual due to their size (table 41.1). Of the ten largest fires on record, two occurred in 1987, and both were caused by lightning.

The years 1987 and 1990 were extreme fire years. The fires during these years were caused primarily by lightning (more than 90% of the area burned due to lightning fires) and were enormous in size (table 41.1). Studying a phenomenon in the immediate aftermath of an extreme event, it is difficult to ascertain the significance of that event in a more global sense. One cannot determine directly whether the event was due to random chance or whether it was a portent of things to come.

In the case of the recent lightning fires, however, clues can be found in the longer-term patterns of human- and lightning-caused fires. While the arithmetic means for the areas burned by human- and lightning-caused fires virtually identical (569 ha and 564 ha [1,405 acres and 1,393 acres], respectively) their distributions are different, as is reflected in their median values (105 ha and 39 ha [259 acres and 96 acres], respectively). Most lightning fires were small, but occasionally they were huge (table 41.1). The trends in the size and occurrence of human- and lightning-caused fires over time were also different. When we compared pre-1940 fire patterns (1908–39) with post-1940 patterns (1940–92), we found that the median size of the largest annual human-caused fire decreased by a factor of 2 in the post-1940 period (table 41.2), as did the median number of fires per year (table 41.2). Conversely, the number of lightning-caused fires, while much smaller, remained constant. Interestingly, this statement is still valid if we eliminate the recent large lightning fires (table 41.2).

It appears, therefore, that fire suppression and possibly public education have had a measurable impact on the characteristics of human-caused fires, but not on those of lightning-caused fires. This may be due to differences in ignition patterns and the necessary response of the fire-suppression organization to lightning and human ignitions. Human-caused fires generally occur as singular events. This allows the fire-suppression organization to respond to individual fires with a large body of fire-suppression resources. Lightning fires, on the other hand, often occur as multiple simultaneous ignitions. In years that are drier than the norm, the amount of resources necessary to deal with simultaneous multiple ignitions can quickly exceed what is available.

These relationships between lightning fires and increased use of resources have been understood for a long time. Because of the 1917 fire season, Show and Kotok (1923) recognized that lightning events have the potential to strain the fire-suppression organization severely. They noted that this was especially true when lightning events were general storms starting multiple fires across the region.

FIGURE 41.4

a, Trends in the number of fires and the acreage burned by the largest fire: the number of fires recorded each year between 1908 and 1992; *b*, the average proportion of the total yearly acreage burned that can be attributed to the largest fire that occurred that year.

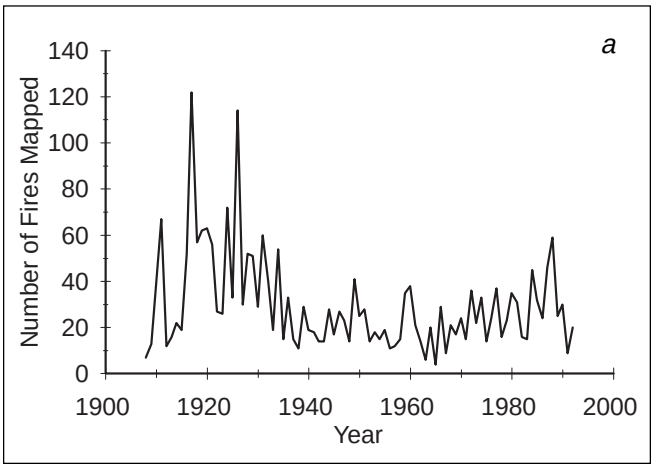

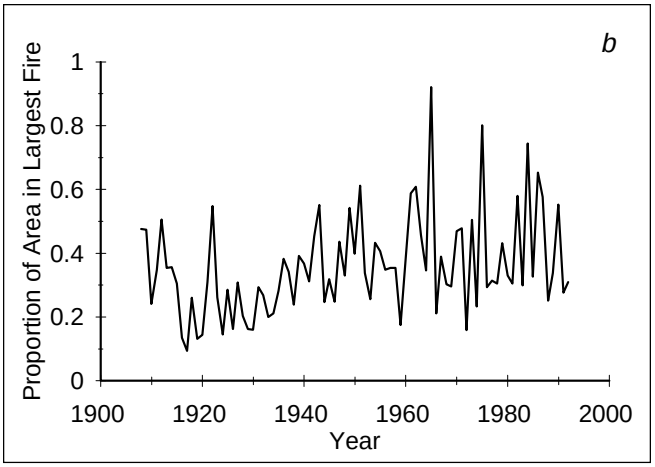

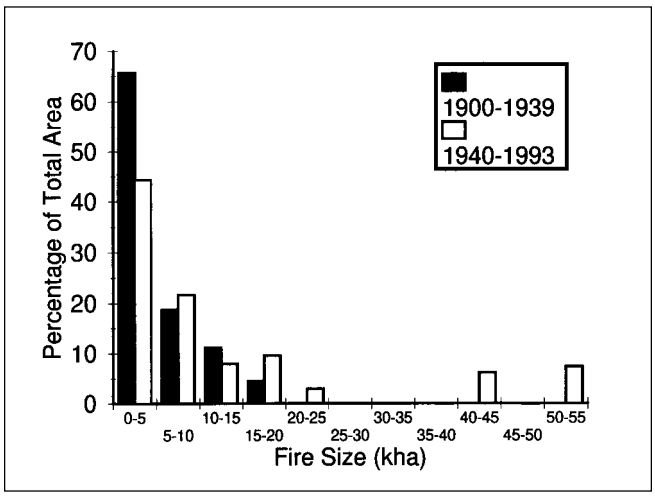

FIGURE 41.5

Proportion of total area burned by fires in different size classes. No fires larger than 20 kha were mapped prior to 1940.

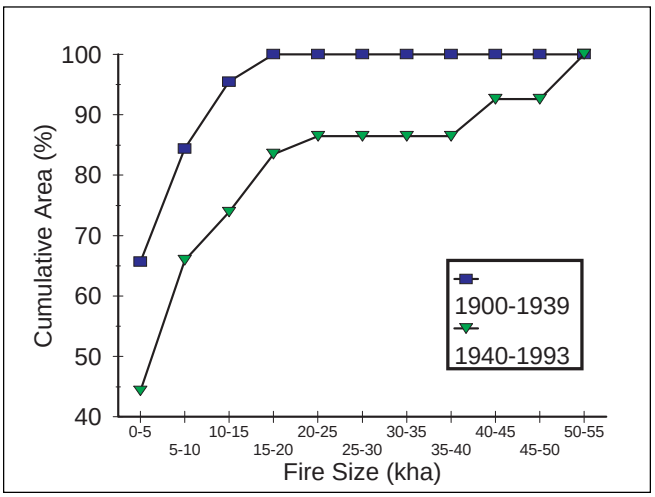

FIGURE 41.6

Cumulative fire area as a function of fire size.

This difference in ignition patterns may explain the observed patterns in human- and lightning-caused fires. Human-caused fires often occur during extreme fire weather, and hence they have a large median size. Because they occur singly, immense resources can be brought to bear. Increased mobility and organizational efficiency have, therefore, produced a decrease in the median fire size for human-caused fires. Because lightning fires involve multiple simultaneous ignitions, the suppression response is more diffuse, and fire behavior becomes more limited by the weather conditions, which are often cool and moist. If, however, major lightning events are coupled with extreme fire weather, they can overwhelm local suppression resources and grow together into "complexes" covering large areas.

EVALUATING LANDSCAPE PATTERNS

Fire is a stochastic event, and fires are discrete spatial events—either an area is within the perimeter of the fire or it isn't. The probability of being in either of these states, for any given location, is dominated by local contagion (Chou et al. 1990, 1993). Evaluation of a single fire, or a small number of fires, therefore, will tell us little about the underlying structural patterns; many fires need to be incorporated into the analysis in order to ascertain whether there are similarities that connect all of the fires to underlying processes.

Because of fire's discrete nature (burned/unburned), a binomial model is natural. However, because the analysis must include many fires, it is necessary to accumulate them over time, and some areas will reburn, leaving the possibility of a

FIGURE 41.7

Acres burned by fires, 1908–92: *a*, caused by humans; *b*, caused by lightning.

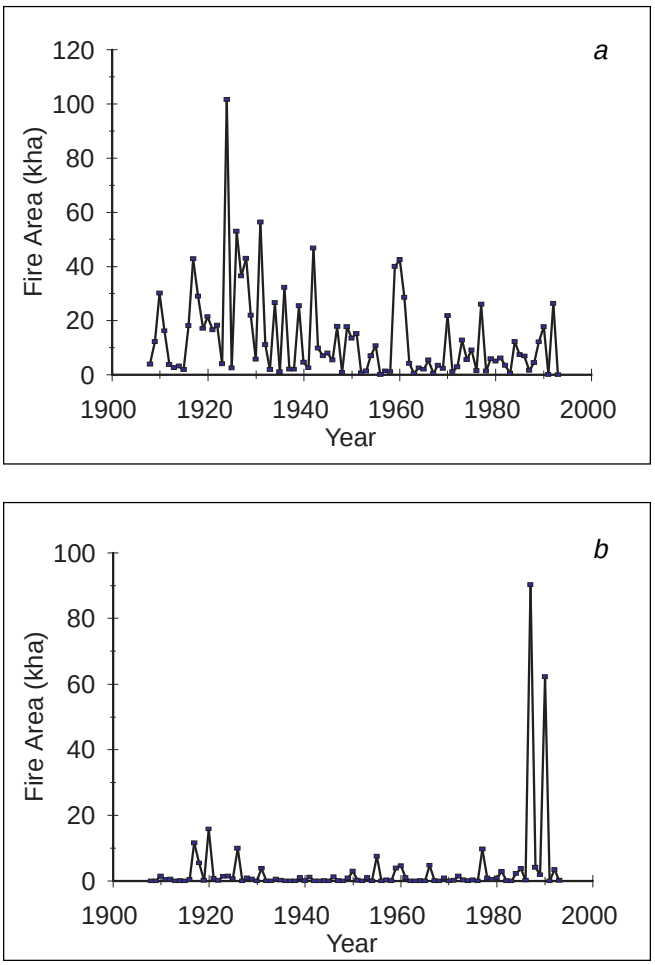

multinomial structure (unburned, burned once, burned twice, etc.). For simplicity, we suppressed the repeated burns and categorized the landscape as either unburned or burned at least once. Using this description, we utilized logistic regression to explore fire patterns.

The need to include many fires, covering extensive domains both in space and time, imposed additional constraints. The analyses required independent variables that were spatially extensive, as well as being reasonably accurate and consistent over time.

Obtaining the Available Data

Because the CALOWL EIS fire maps (USFS 1996) were collated for fires on or adjacent to national forest lands in the Sierra Nevada, our initial data set was confined to the area described by these maps (figures 41.8 and 41.9).

When the mapped fires were overlaid on national forest ownership boundaries, however, approximately 40% of the fire area was exterior to U.S. Forest Service (USFS) land. To include acreage exterior to USFS lands, a new map boundary was required. This boundary needed to incorporate as much of the fire area as possible without extending so far beyond USFS boundaries that fire frequency would be controlled by a lack of reporting rather than a lack of fire. To achieve this we arbitrarily buffered USFS land boundaries by 2,000 m (6,600 ft), enclosing approximately 50% of the exterior fire area.

To describe the fire patterns in terms of other descriptive variables, we needed spatially referenced data that covered this same region. Topographic data were available through a 100 m (330 ft) Digital Elevation Map (DEM) compiled by the SNEP Geographic Information System (GIS) center (plate 41.1). Slope, aspect, and elevation were, therefore, available at 1 ha (2.5 acre) resolution across the entire region.

For these analyses, the DEM-derived data were modestly manipulated. Examination of the DEM showed that it was "banded" in the north-south direction (banding is a data artifact common to DEMs). Because both slope and aspect are sensitive to banding, we applied a 3x3 focal mean function to the DEM to remove these artifacts (Brown and Bara 1994). Aspect and slope were then generated using standard Arc/Info (Environmental Systems Research Institute Inc., Redlands, California) GRID functions.

Aspect is undefined for flat areas (and unreliable in areas of minimal slope) and is a circular statistic. For fire, aspect should be related to potential evapotranspiration (PET), which is a function of both temperature and radiant energy (Campbell 1977). South-facing slopes and flat areas receive the most sun, but the temperature maximum occurs after solar noon. Hence, the peak PET will occur on flat areas and southwest (SW) slopes. Fire studies have found that fire occurrence conforms to these understandings (Agee et al. 1990), with the highest fire frequencies on SW aspects. We therefore used these understandings to develop a simple transform of aspect, using angular distance from south-southwest (SSW) (203°) as a metric. SSW aspects, therefore, were given a value of 0, and north-northeast (NNE) aspects had a value of 180. Flat areas (defined as areas with slopes of less than 10%) also received a value of 0.

In addition to slope, aspect, and elevation, there are significant differences in rainfall between the northern and southern Sierra. To capture these differences, we obtained a digital copy of an isohyetal map developed by the U.S. Geological Survey (plate 41.2) (Rantz 1969). This map covers only the state of California and therefore precluded analysis on those areas where USFS lands, or our buffer, extended into Nevada.

Lastly, we removed all large bodies of water from the map, using the CALVEG (Matyas and Parker 1979) water layer.

TABLE 41.1

The ten largest mapped fires, 1900–1993. All of the large lightning-caused fires occurred in 1987 and 1990. Two of these are the largest fires on record and are more than twice the size of other large fires.

Year	Size (ha)	Cause	Rank
1924	15,055	Human	9
1931	17,715	Human	5
1942	21,234	Human	3
1960	18,100	Human	4
1960	17,057	Human	7
1961	17,459	Human	6
1987	53,011	Lightning	1
1987	16,152	Lightning	8
1990	44,272	Lightning	2
1990	14,508	Human	10

TABLE 41.2

Median values for annual fire data. The period 1940–86 is included here to remove the impact of recent large lightning-caused fires.

	Time Period			
	1908–92	1908–39	1940–92	1940–86
Maximum Annual Fire Size (ha)				
All causes	2,588	4,406	2,199	2,154
Lightning	217	215	217	172
Human	2,525	4,406	1,881	1,881
Number of Fires per Year				
All causes	24	33	21	20
Lightning	4	4	5	4
Human	18	31	16	16

Developing a Logistic Function to Describe Burn Patterns

To relate fires to topography and vegetation, Chou et al. (1990, 1993) divided the landscape into irregular polygons based on topography and utilized values associated with each poly-

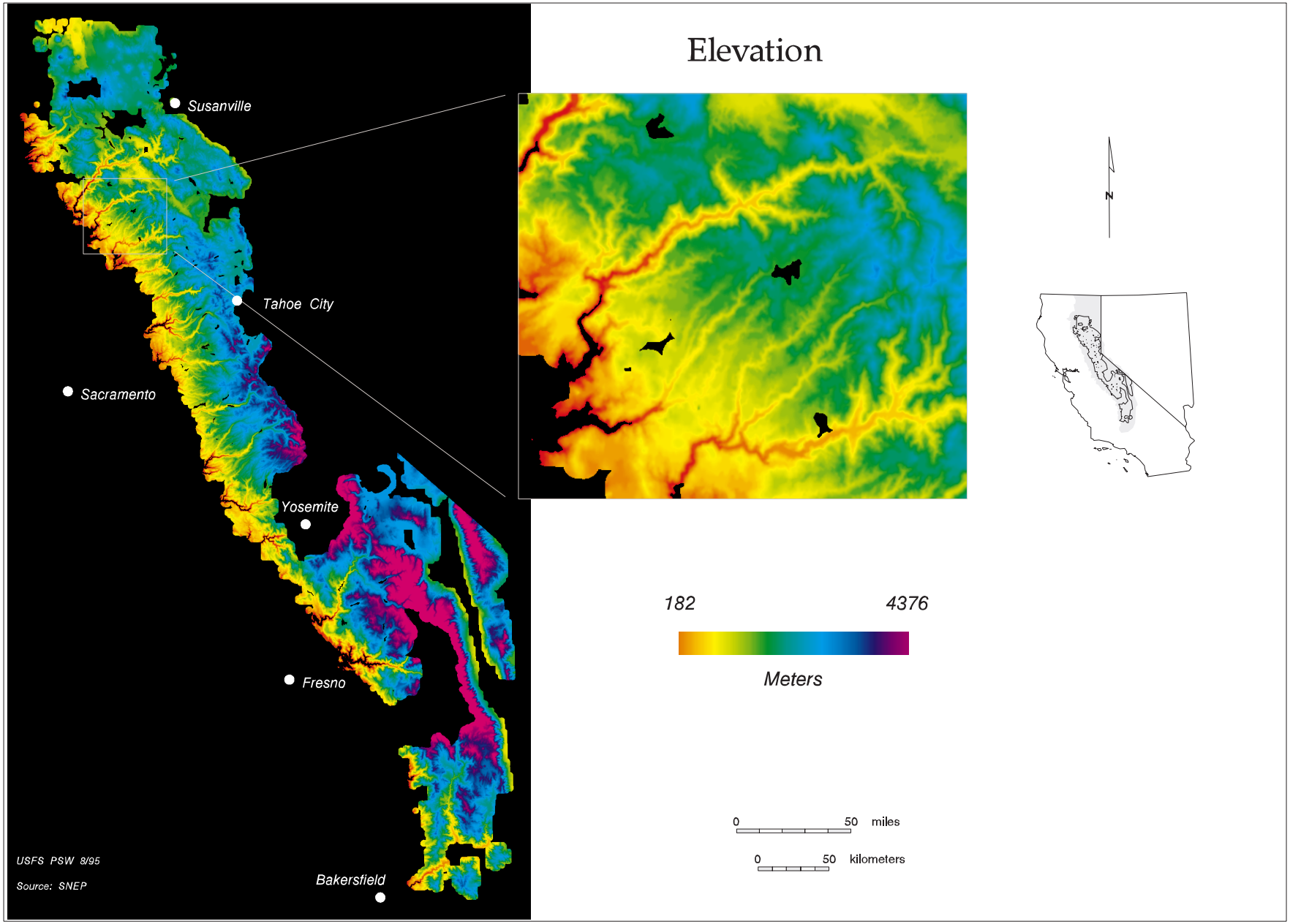

PLATE 41.1

The elevation surface used to generate slope, aspect, and elevation for analysis of fire patterns. Elevation data are spaced 100 m (330 ft) apart, giving the map 1 ha (2.5 acre) resolution.

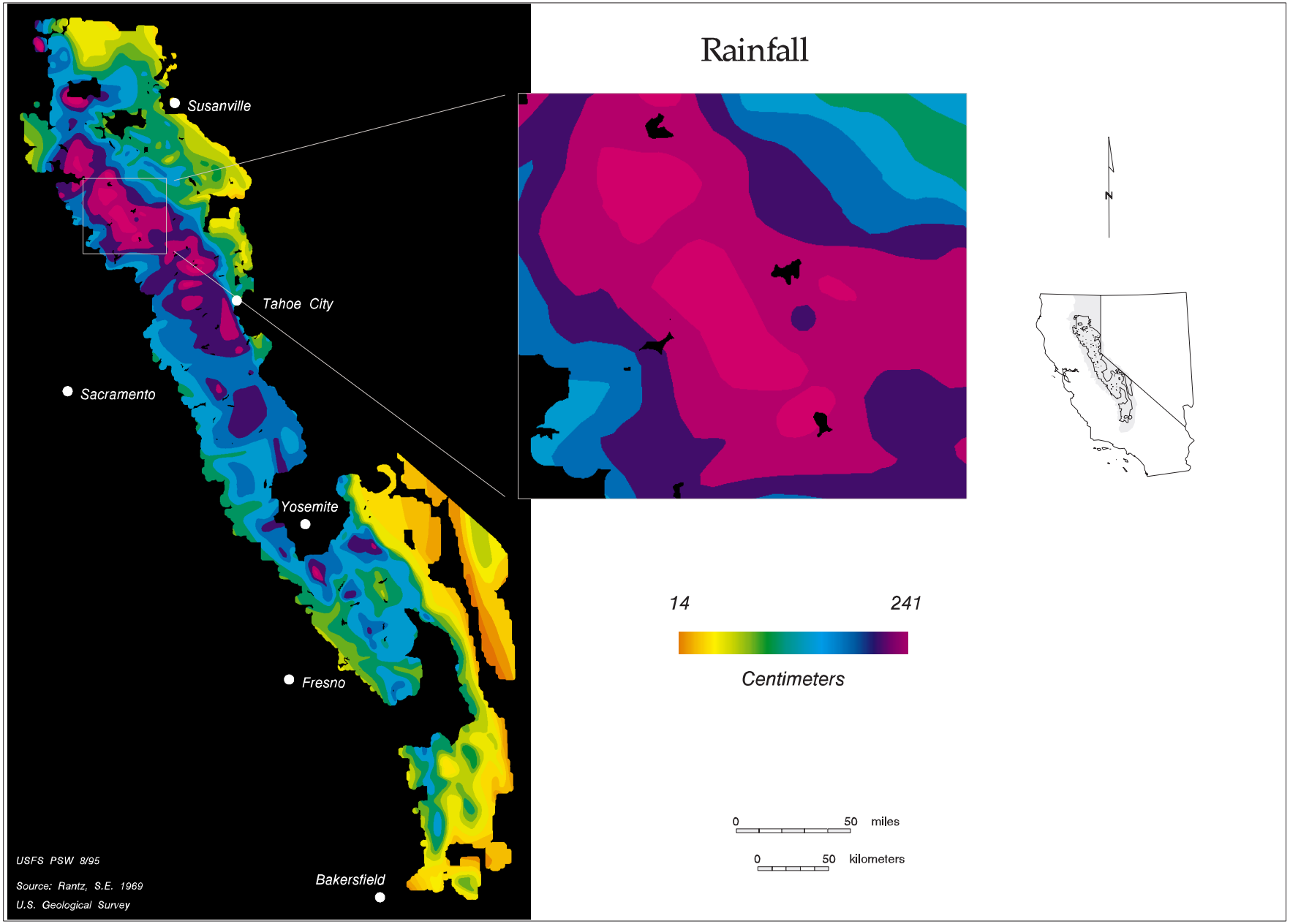

PLATE 41.2

Isohyetal map of precipitation patterns. Rainfall increases in the northern Sierra, whereas the highest elevations are in the south (adapted from Rantz 1969).

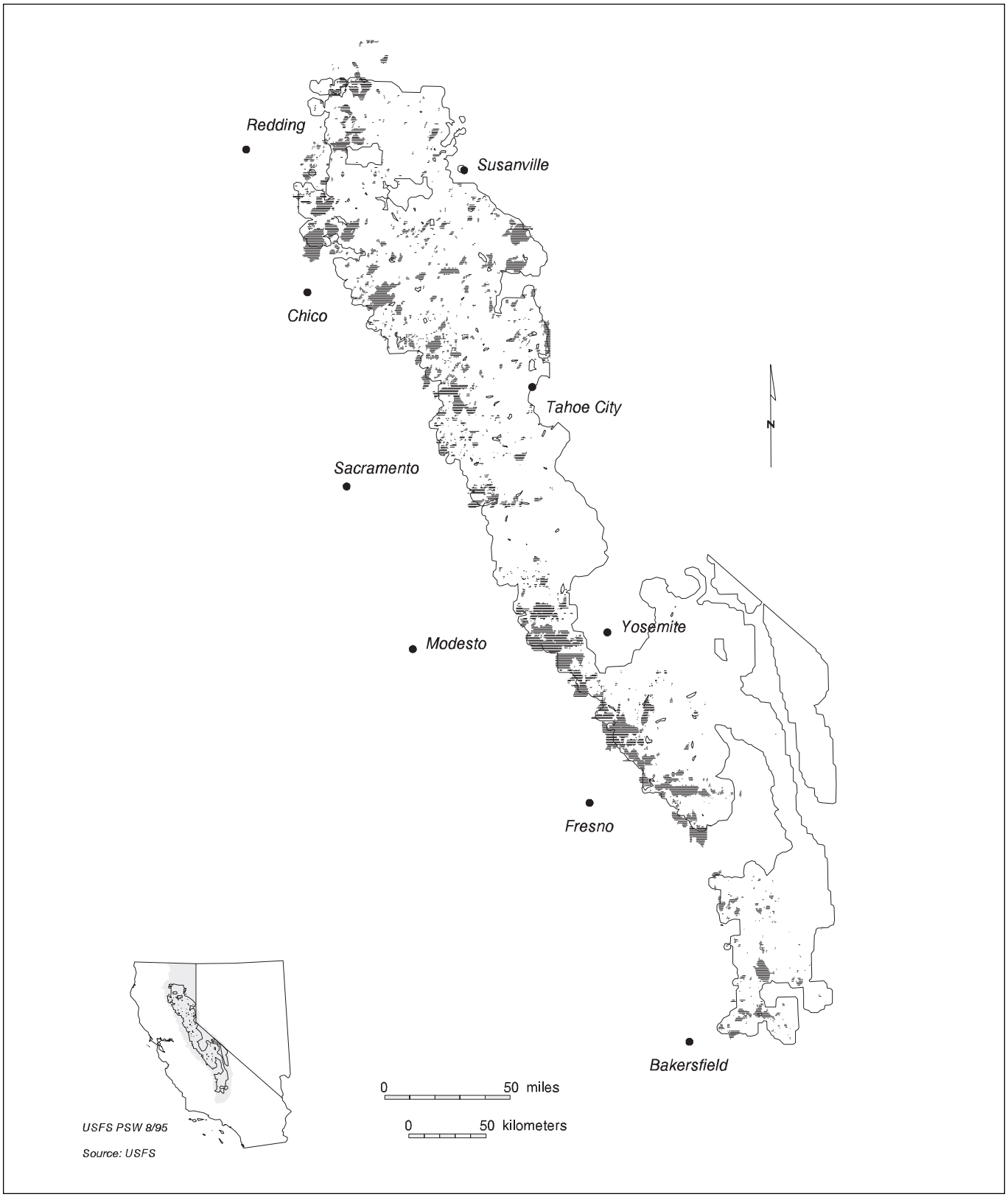

FIGURE 41.8

Map of fires (1900–1939) on and around U.S. Forest Service lands. The analysis area is overlaid on the mapped fires, and any fire area exterior to the study area was excluded from the landscape analyses (adapted from USFS 1996).

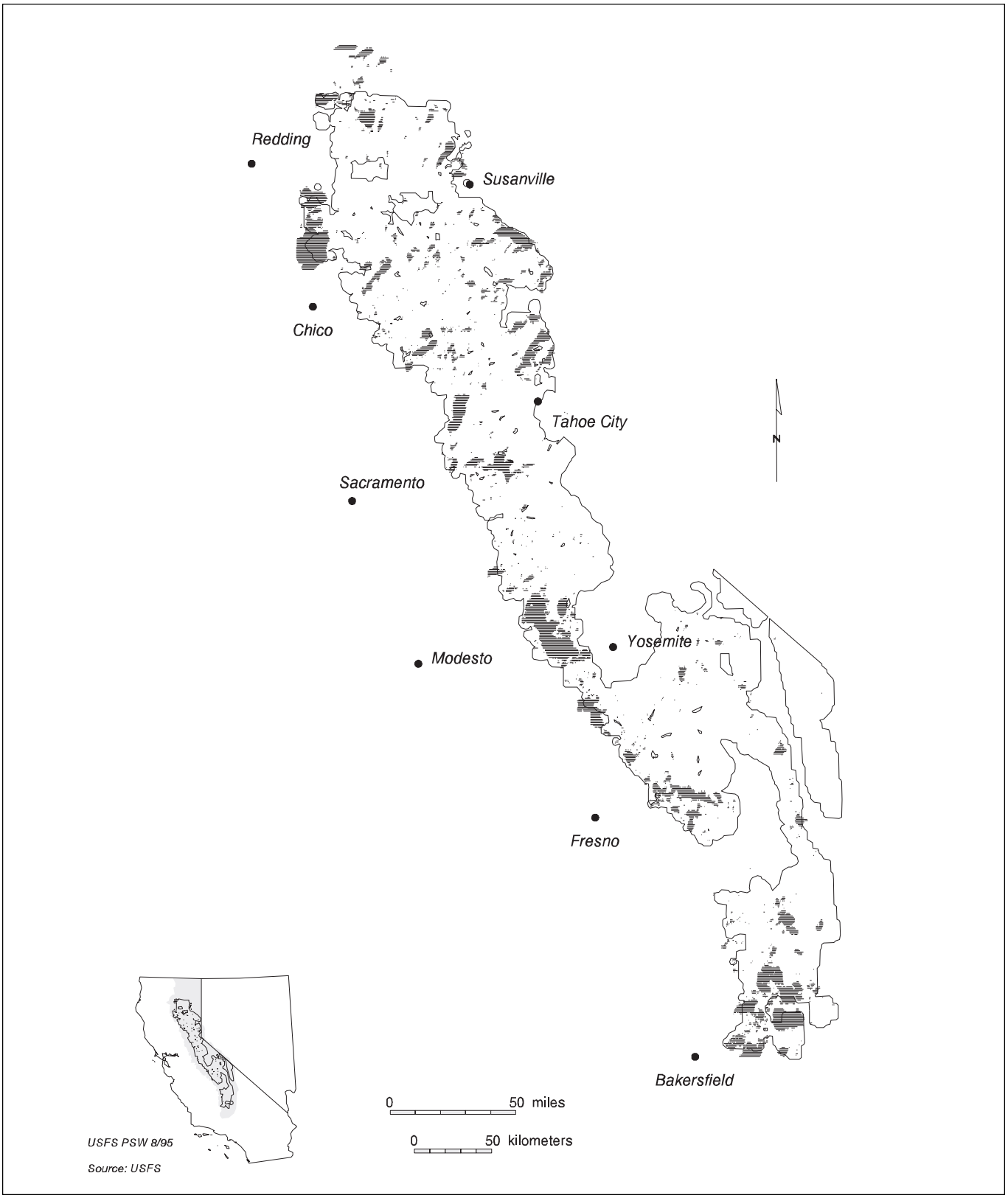

FIGURE 41.9

Map of fires (1940–93) on and around Forest Service lands. The analysis area is overlaid on the mapped fires, and any fire area exterior to the study area was excluded from landscape analyses (adapted from USFS 1996).

gon to develop regression functions. We chose to use attributes of sample points randomly located on the landscape or, more precisely, individual grid cells (1 ha [2.5 acres]) as if they were point locations on the landscape. This approach has a number of advantages over the use of polygons, obviating the need for variables such as area and perimeter. The number of sample points used for regression was quite arbitrary (we had access to the entire landscape of 5.7 million cells). We chose 32,000 random cell locations and obtained their slope, aspect, elevation, rainfall, location (Universal Transverse Mercator [UTM]), and information regarding whether they had been burned during the time periods 1900–1939 (pre-1940), 1940–93 (post-1940), or at all during the time period 1900–1993 (all). For these analyses, 1940 is a logical break point because approximately half the area burned prior to 1940 (figure 41.3). We used the S-Plus (MathSoft, Inc., Seattle, Washington) statistical package to perform the logistic regressions.

Three models were developed, originally using all available independent variables. Fires were grouped into pre-1940, post-1940, and all. In all three models, the dominant factors controlling fire frequency were elevation, slope (steeper slopes burned more frequently), and rainfall (drier areas burned more frequently) (table 41.3). Of these three, elevation was by far the most important. Aspect had little impact on fire frequency. Formal significance tests on the regression coefficients were not warranted, as the sample size was arbitrary. However, because the sample size was large (32,000 points), the expectation was that all relevant variables would have large t-values.

Choosing a Model

Because elevation dominated the regression equation, we evaluated fire-frequency patterns over time as a function of elevation. When the proportion burned within 100 m (330 ft) elevation bands was compared, pre-1940 and post-1940 fire patterns were very similar (figure 41.10), with burn frequency increasing with decreasing elevation to about 500 m (1,650 ft) and then declining. The decrease in burn frequency below 500 m is almost certainly unreliable. An examination of the map (plate 41.1) showed that areas below 500 m elevation were confined to deep inner gorge areas of major rivers and represented only 0.7% of the map area. We therefore do not feel that the frequency data for these elevation zones should be extrapolated to the general lower foothills zone, which is largely exterior to our study area.

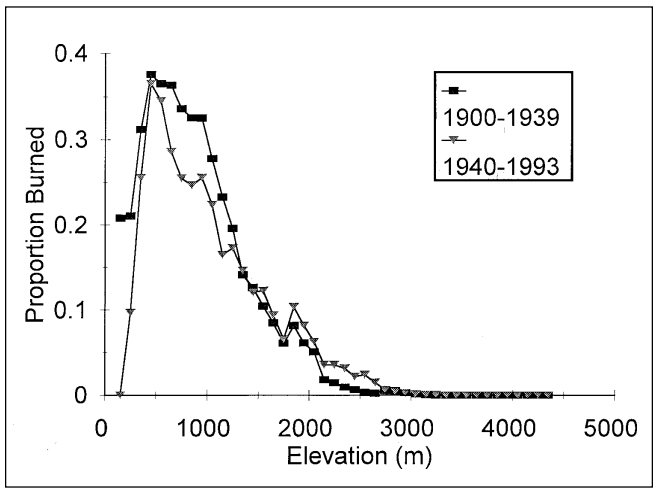

FIGURE 41.10

Proportion of 1 ha (2.5 acre) cells that burned, binned into 100 m (330 ft) elevation zones. Elevations below 500 m (1,650 ft) represent a tiny proportion of the study area and are confined to the inner gorges of major rivers.

The cumulative acreage distributions were also very similar, with the median elevation for each distribution lying between 1,000 m and 1,500 m (3,300 ft and 4,950 ft) (figure 41.11). Based on these data, it is reasonable to state that fires throughout the twentieth century in the Sierra Nevada have occurred within similar elevation zones and that the proportions burned have not varied appreciably.

Because there is very little difference between pre- and post-1940 fire patterns, and because the model was stronger when all fires were included, a model utilizing the entire fire record and including elevation, slope, and rainfall was chosen as an appropriate model to describe fire frequency in the Sierra Nevada (table 41.4).

TABLE 41.3

Logistic regression models for fire frequency. The All Fires columns show the acres that burned at least once across the entire period. Row is a proxy for latitude and equals 1 at the northern end of the map and 6,400 at the southern end.

	Pre-1940		Post-1940		All Fires	
	Coefficient	*t*-value	Coefficient	*t*-value	Coefficient	*t*-value
Intercept	7.045E-1	7.6	7.467E-1	8.4	1.785	23.8
Elevation	–1.971E-3	–49.8	–1.560E-3	–44.2	–1.922E-3	–61.1
Slope	1.470E-2	5.4	2.987E-2	11.7	2.605E-2	11.8
Rainfall	5.769E-4	1.2	–7.581E-3	–16.1	–4.250E-3	–11.5
Aspect	2.200E-4	0.6	–1.055E-3	–2.8	–6.719E-4	–2.1
Row	–2.026E-5	–1.5	2.644E-5	2.1	8.021E-6	0.8

Testing Model Fit

We tested the fit of the model by binning the landscape into deciles of risk based on model predictions (Hosmer and Lemeshow 1989, 142). Hosmer and Lemeshow (1989) present a statistic closely related to X^2 to evaluate the quality of this fit, but, as we mentioned before, our sample size is arbitrary and significance tests are artificial. However, because we had access to the entire population of cells, we directly assessed the quality of fit by using the following method:

1. For each grid cell on the map (approximately 5.7 million locations), we computed the model estimate of fire probability and assigned the cell to a decile based on this estimate.
2. For each decile, we accumulated the model estimates, the number of cells which burned, and the total number of grid cells.

We were then able to compute the ratio of burned to unburned cells (the actual frequency for that decile) and compare it with the model estimate,

$$M_j = \frac{\sum_{i=1}^{t_j} E\ (y | e_{i,j}, s_{i,j}, r_{i,j})}{t_j} \qquad (1)$$

where M_j is the model estimate for decile j, t_j is the total number of cells in the decile, and $e_{i,j}$, $s_{i,j}$, and $r_{i,j}$ are the elevation, slope, and rainfall evaluated for cell i in decile j.

This test is a strong validation of the quality of the model as a descriptor of historic fire frequency because the results are an exact statement of the relationship between the model and the surface it is supposed to represent. For purposes of developing a fire-risk map, the test is particularly appropriate: For a particular area of the map, if the model predicted a particular fire frequency, how close to this estimate was the actual historical fire frequency evaluated within that same area?

This test was performed for all fires, using the final model (table 41.4). The match was very close for deciles 0–10 through 50–60 (figure 41.12), but the model overestimated fire in the higher fire-frequency deciles. The total acreage in these higher deciles, however, was tiny (figure 41.12), and the model was therefore insensitive to these divergences. To correct this problem, we simply truncated the model estimates at 60% (in essence creating a 60+ bin). When this was done, the model estimates conformed to the measured frequencies very closely (plus or minus 2.5%) for all deciles (figures 41.13 and 41.14).

Testing model fit in logistic regression is generally done at the decile level, probably because small sample size precludes

TABLE 41.4

Logistic regression model based on all fires and excluding aspect and row. This model, with the provision that model estimates would be truncated at 60%, was used to generate a fire-frequency map for the Sierra Nevada.

	All Fires	
	Coefficient	***t*-value**
Intercept	1.803	27.8
Elevation	–1.925E-3	–61.2
Slope	2.436E-2	13.0
Rainfall	–4.375E-3	–13.1

FIGURE 41.11

Cumulative acreage burned, by elevation. The arrows point to the median elevation (half the fire area is below, half above this point) for each curve.

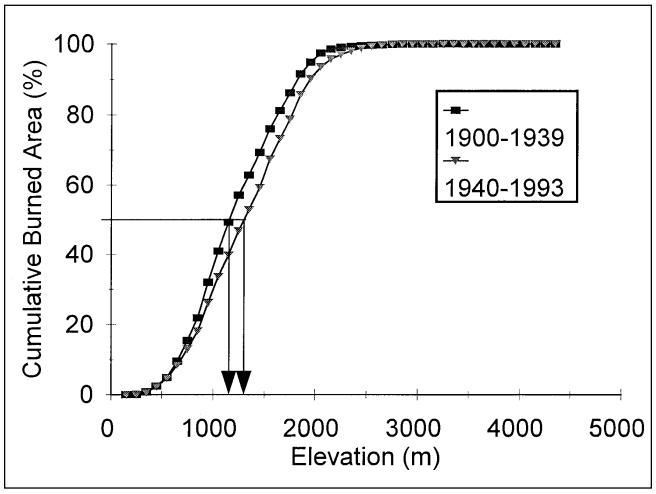

FIGURE 41.12

A test of model fit to actual burn patterns based on risk deciles (10% bins). The model overestimates fire probability for high-risk zones.

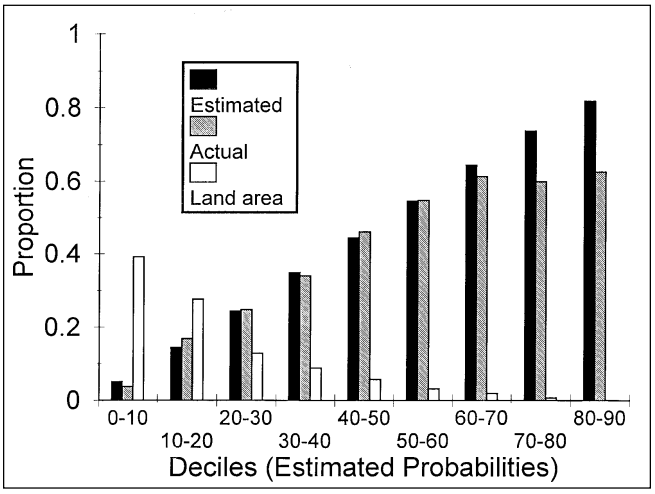

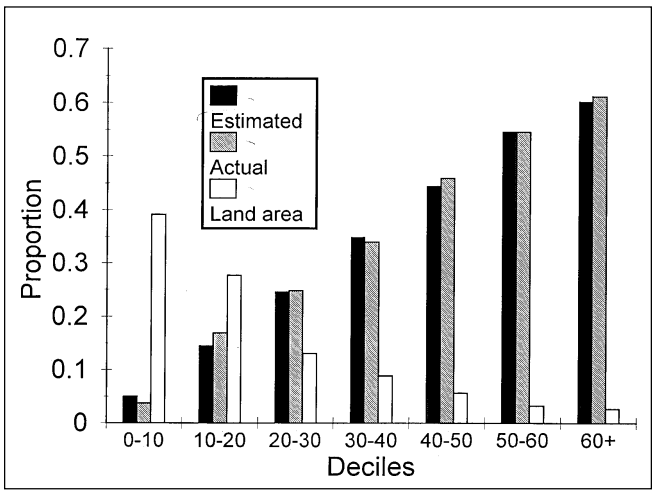

FIGURE 41.13

A test of model fit to actual burn patterns based on risk deciles (10% bins), but with model estimates greater than 0.6 combined into a single bin.

finer groupings. Here, however, we were able to test the model at a finer scale. When binned into groups of 1% (centiles), the model fit was still reasonable (figure 41.15). Deviation between model estimates and measured fire frequencies was within 4% for all centiles.

Developing a Risk Map

Because the model accurately described the probability of fire, we generated a generalized fire-probability map by computing the model estimates for each grid cell (plate 41.3). Because the fit to historical patterns was good, and because these burn patterns remained remarkably constant over time, we feel that it is reasonable to use this map to evaluate relative fire risk in the near future for specific locations.

Estimating Fire Frequency Based on Vegetation Types

Vegetation was excluded from the logistic regression analysis just described for a number of reasons, the most important of which is that vegetation is not static on the landscape. An area currently mapped to a vegetation type may not have been that same type when a fire occurred. In fact, the area may be in its current condition because of its past fire history. Vegetation may, however, be less abstract than a multidimensional topographic model, and the burn patterns linked to vegetation types may give insights that are missed in the topographic analysis.

The vegetation map covering the analysis area available to us was the CALVEG map (Matyas and Parker 1979). When we looked at fire patterns within each CALVEG vegetation stratum, we found that the strata with the highest proportions burned were generally associated with the west-side foothills (table 41.5). The highest rates of burning occurred in the interior live oak and blue oak types, with the next two highest levels in chaparral types. The fire frequencies associated with these types were at or above (mostly above) the fire frequencies associated with the arithmetic-mean elevation of each type (figure 41.16). The elevation trend for these fire-prone strata, however, followed the general elevation trend—strata with higher mean elevations burned less frequently (figure 41.16).

FIGURE 41.14

Deviation between the model and the actual fire distribution for each risk decile (10% bins). This is not a statistical measure but rather an exact statement of the divergence between model expectations and the patterns upon which the model is based.

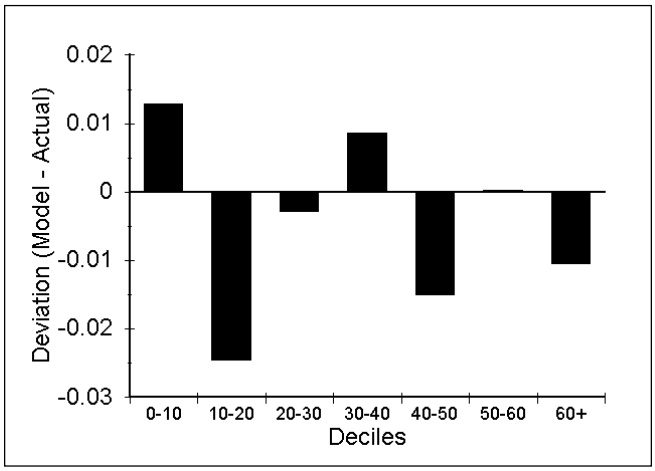

FIGURE 41.15

Deviation between the model and actual fire distribution for risk centiles (1% bins). The actual proportion burned is compared with weighted model estimates for each centile.

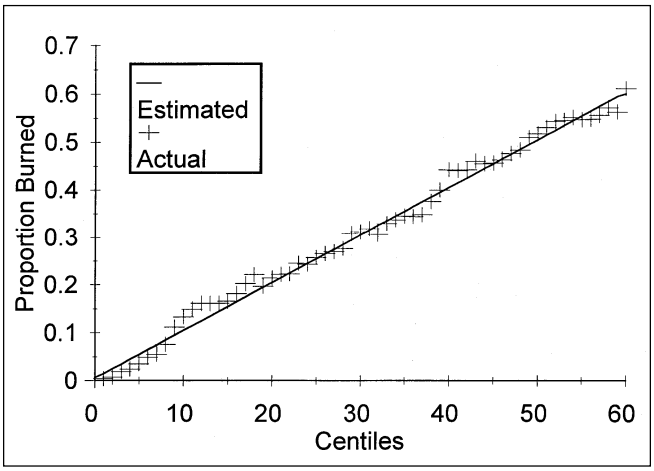

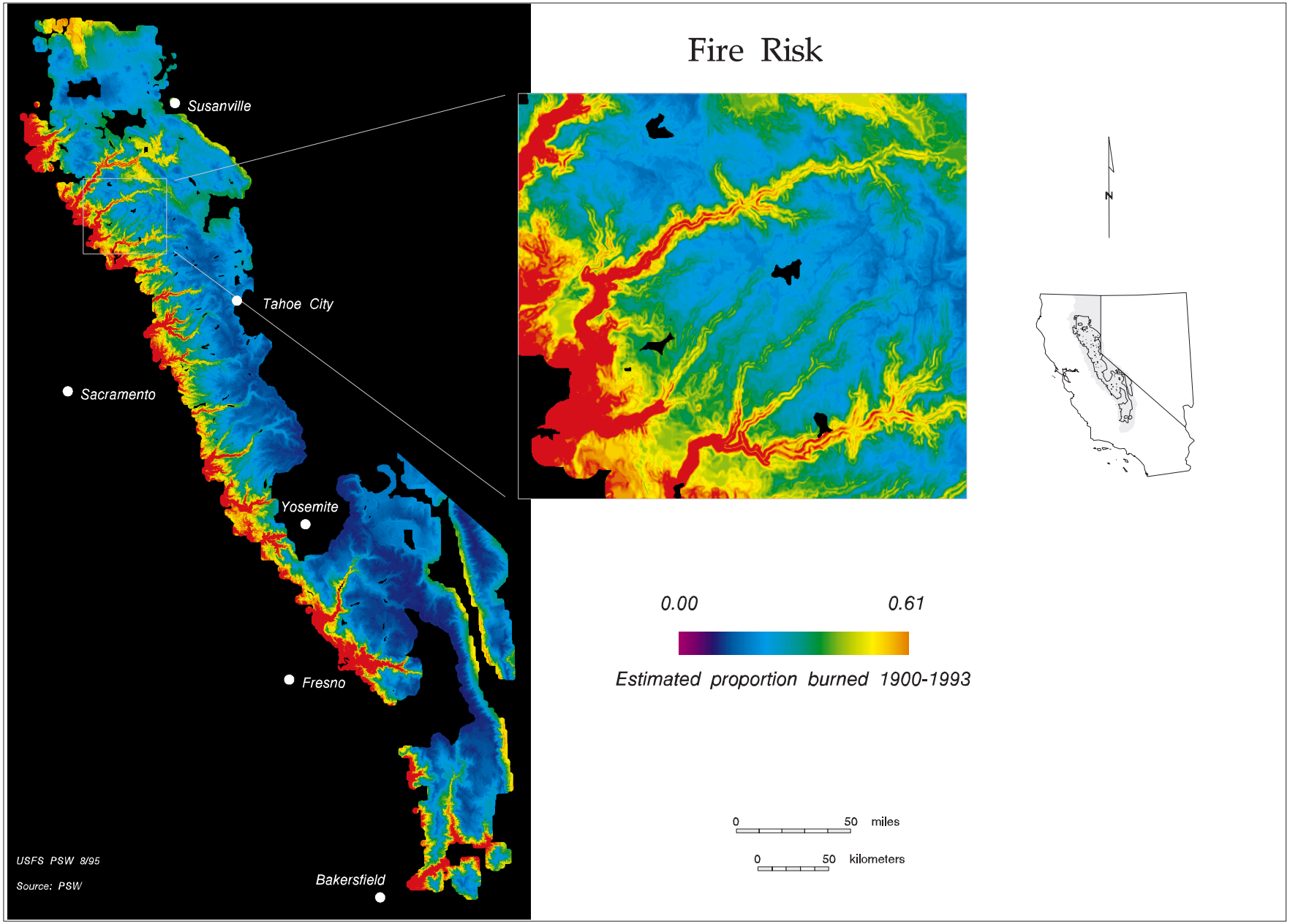

PLATE 41.3

Map of model expectations for fire frequency for the entire study area. Risk levels were based on fire frequency for the period 1900–1993, using elevation, slope, and rainfall as independent variables.

TABLE 41.5

Fire frequencies for selected CALVEG vegetation strata in the Sierra Nevada. Strata larger than 10,000 ha and with more than 30% of the strata burned at least once were selected. If the estimated fire rotation exceeds the measured one, the strata reburn more frequently than would be expected based on random fire patterns.

Strata name	Area (ha)	Area Burned[a] (ha)	Proportion Burned[b]	Measured Fire Rotation[c] (Years)	Estimated Fire Rotation[d] (Years)
Interior live oak	21,673	16,509	0.76	57	59
Blue oak	84,417	59,092	0.70	78	70
Chamise	111,307	64,389	0.58	114	98
Whiteleaf manzanita	91,031	42,464	0.47	106	133
Ponderosa pine	332,974	112,869	0.34	192	205
Mixed conifer–pine	699,740	235,251	0.34	185	208
Canyon live oak	102,445	32,222	0.31	189	223

[a]Area burned at least once based on the CALOWL EIS fire map.
[b]Proportion burned at least once based on the CALOWL EIS fire map.
[c]Based on total area burned/total strata area, for the period 1908–92.
[d]Based on the Poisson expectation, λ/t, where $t = 85$ years.

EVALUATING REBURN PATTERNS

The Poisson Model

If planar shapes (disks, for instance) are randomly scattered on a surface, the areas of overlap will approximate a Poisson distribution (see Horn 1971, chapter 5):

$$P(k,\lambda) = e^{-\lambda}\frac{\lambda^k}{k!} \qquad (2)$$

where k is the number of disks that overlap on a specific location and λ is combined projection area of all of the disks. Given $P(0,\lambda)$, the probability that a site is not covered by any disks, equation 2 simplifies to

$$P(0,\lambda) = e^{-\lambda} \qquad (3)$$

and can be solved for λ by taking logarithms.

This approach can be used to test for the random placement of fires (Agee 1993). If fires occur randomly on the landscape, the reburn patterns will follow Poisson expectations.

We know, based on the logistic regression described previously, that in a global sense fires are not randomly distributed on the landscape. Slope, elevation, and rainfall determine their likelihood. Hence, globally we can reject the expectation of randomness. Of more interest, given that there is a zone of equal fire probability (that is, $P(0,\lambda)$ is constant), is the question, Is the reburn pattern random within that zone? This question is important both for ecological reasons and for controlling fire. If reburn patterns deviate significantly from a random pattern, we can use the specific fire history for a site to modify local risk assessment.

The logistic regression described earlier developed fire-expectation functions based on whether a site had never burned in the twentieth century or had burned at least once. The frequency-of-burning statistics produced by the regression are, therefore, equivalent to $(1\text{-}P(0,\lambda))$. Because the model does a good job of predicting $(1\text{-}P(0,\lambda))$, we can use the model to bin the map into equal risk zones (the deciles in figure 41.13) and compute $P(0,\lambda)$ directly for each bin as fraction of cells in the bin which did not burn (based on the "actual" bars in figure 41.13). Solving for λ, given $P(0,\lambda)$, we can then use equation 2 to estimate $P(1,\lambda) \ldots P(n,\lambda)$ where (1..n) is the number of times that a site reburned during the time period and assuming a random spatial location for all burned cells. We can then compare the actual distributions of reburns and determine whether they conform to Poisson expectations.

If sites burn more frequently than expected, estimates for $P(1,\lambda)$, and possibly $P(2,\lambda)$ in high-risk areas, will be lower than the measured frequencies, and $P(3,\lambda) \ldots P(n,\lambda)$ will be higher. If sites reburn less frequently than the random model, this pattern will be reversed.

FIGURE 41.16

All of the CALVEG classifications for which more than 30% of the area burned at least once, based on all mapped fires. The bars are placed at the arithmetic mean elevation for each vegetation type, rounded to the nearest 100 m, and the line is the proportion of the landscape that burned at that elevation.

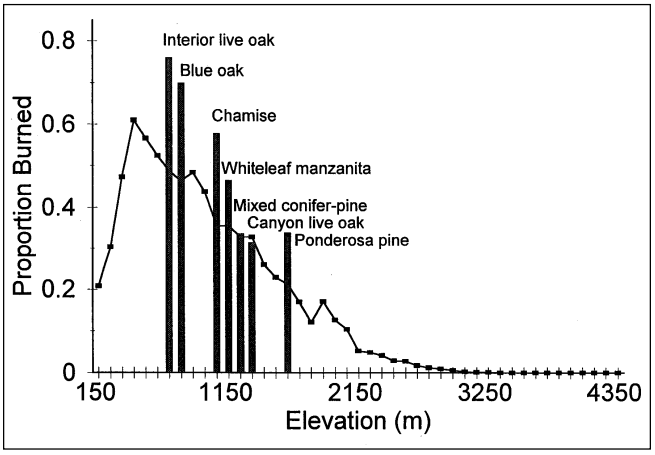

Evaluating Reburn Patterns

Based on this logic, we broke the landscape into deciles of fire risk based on the logistic regression described previously (figure 41.13), counted the proportion of cells in each bin that had burned 0..*n* times, computed λ and the expected proportions (1..*n*) based on the Poisson distribution, and compared the measured reburn patterns with Poisson expectations. A X^2 test is often used to evaluate fit to the Poisson distribution (Feller 1968). In this case, however, this test is inappropriate due to the large and arbitrary size of the sample (see Wonnacott and Wonnacott 1977, pgs. 506–507). The actual *n* is related to the number of fires (2,536) and their acreage distribution rather than to the number of sample points. However, determining the relationship of these fires to individual decile bins was difficult because individual fires crossed multiple bins. We therefore present these data without statistical measures of fit. As was the case with the validation of the logistic regression, these relationships are exact statements of the relationship of a predictive model (in this case the Poisson distribution) to the measured landscape patterns.

Figure 41.17 presents the results of these comparisons. P(0,λ) is directly computed from the map frequency and, therefore, is always exact. In general, the distributions conform reasonably closely to the Poisson distribution. The Poisson model overestimates P(1,λ) and underestimates P(3,λ) to P(8,λ) for all deciles—areas reburn more frequently than would be expected if the fires were random. For the highest risk decile, P(2,λ) is also overestimated. A reasonable way to simplify these patterns is to look at the fire rotation within each decile. This can be computed directly as

$$R_d = \frac{t}{\sum_{k=1}^{n_d} kp_{k,d}} \qquad (4)$$

where R_d is the fire rotation for decile *d*, *k* is the number of times a site was burned, $p_{k,d}$ is the proportion of decile *d* that burned *k* times, and *t* is the elapsed time. This statistic is sometimes referred to as the natural fire rotation (Agee 1993, 100). R_d can also be estimated from the Poisson distribution as λ / t (Feller 1968, 152–53). λ / t overestimates fire-return periods for all decile classes (table 41.6).

While the reburn patterns are not strictly random, the divergences from Poisson expectations are modest and affect remarkably little acreage in the Sierra (figure 41.18). A model that assumed simple random fire patterns within each decile would produce fire patterns extremely close to those observed.

Possible Explanations for the Observed Reburn Patterns

The consistency of divergence from Poisson expectations for all reburn classes and all bins makes it unlikely that this deviation is due purely to chance. This suggests that areas that have a record of frequent fires in the past are somewhat more likely to burn again than areas of similar elevation, slope, and rainfall that have not burned. A number of potential processes could account for these patterns. Previous fire could make a site more flammable through changes in vegetation and fuel loadings. An alternate explanation is that flammability remains constant and that some locations have higher ignition rates. Due to the small areas involved (of the 1.4 million ha that burned, 3 ha [7.5 acres] burned nine times), it is difficult to determine which explanation might be more correct, but an examination of the maps suggests the second. Areas that burn repeatedly appear to be ones that we would identify as high-risk sites (low elevation, steep slopes) that are adjacent to major highways. The canyon wall on the north side of the Merced River (plate 41.4) is a good example. Not only is this area identified as being in a high-risk zone, but a major highway into Yosemite National Park (State Highway 140) runs along the base of the high reburn zone.

Interestingly, there is no evidence that areas that have burned in the past are less likely to burn in the future, as might be the case in a fuel-limited system (Minnich 1983). All of the calculated reburn intervals are, however, longer than eighty years (table 41.6), and it is probable that, for fuels to limit fire acreage, fires would need to burn far more frequently than the observed pattern. This is an important understanding, because the area burned in the twentieth century is not insignificant. The total fire acreage in the CALOWL EIS (USFS 1996) fire map is 1,441,549 ha (3,562,068 acres). In the two zones with the highest fire frequency (more than 50% burned this century), 177,050 ha (437,313 acres) have burned during the period for which we have records, producing 3 ha (7.5 acres) that burned nine times and 116 ha (286 acres) that burned eight times. If we had systematically burned this zone on a ten-year cycle in order to reduce fuels, we would have burned approximately 2.6 million ha (308,299 ha x 8.5) (6.4 million acres) over the same time period—more than fifteen times the amount burned in wildfires.

Another interesting aspect of these analyses is that while, in a broad sense, fire patterns are described by elevation and climate, the patterns of fire overlap are very complex on any smaller scale (plate 41.4). Because the overlap patterns appear to conform reasonably well to a random model, we conclude that most of the overlap within a specific risk zone is due to chance. This provides a cautionary note to descriptions of "average" fire return evaluated either on a site-specific basis or on a limited and nonrandom sample. The expectation is that many sites will have burned more frequently (as well as less frequently) than expectation due simply to chance.

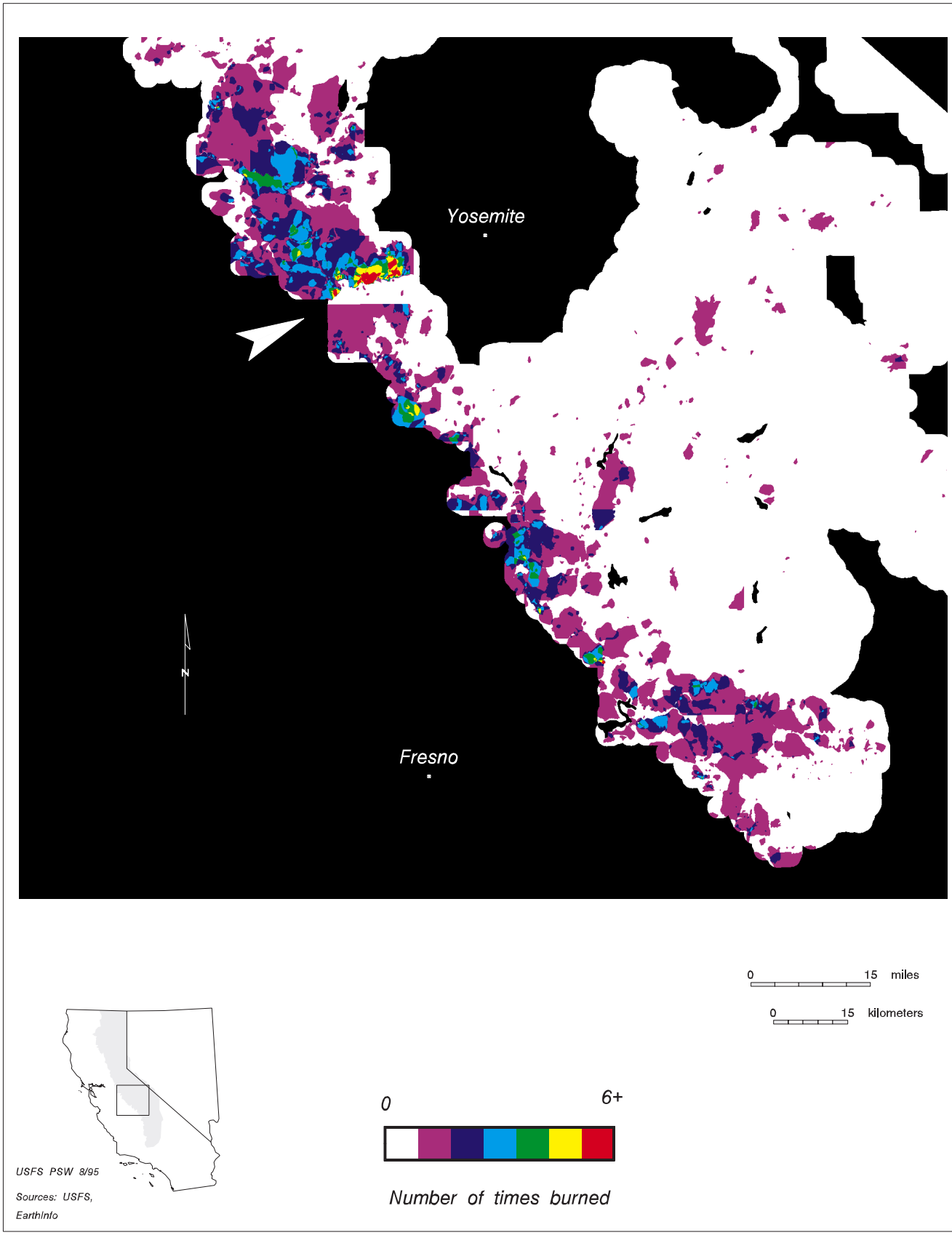

PLATE 41.4

An area of high fire activity in the southern Sierra Nevada. The area, which reburned more than 5 times, is confined to a small section on the north side of the Merced River, immediately adjacent to State Highway 140, a major route into Yosemite National Park (see arrow).

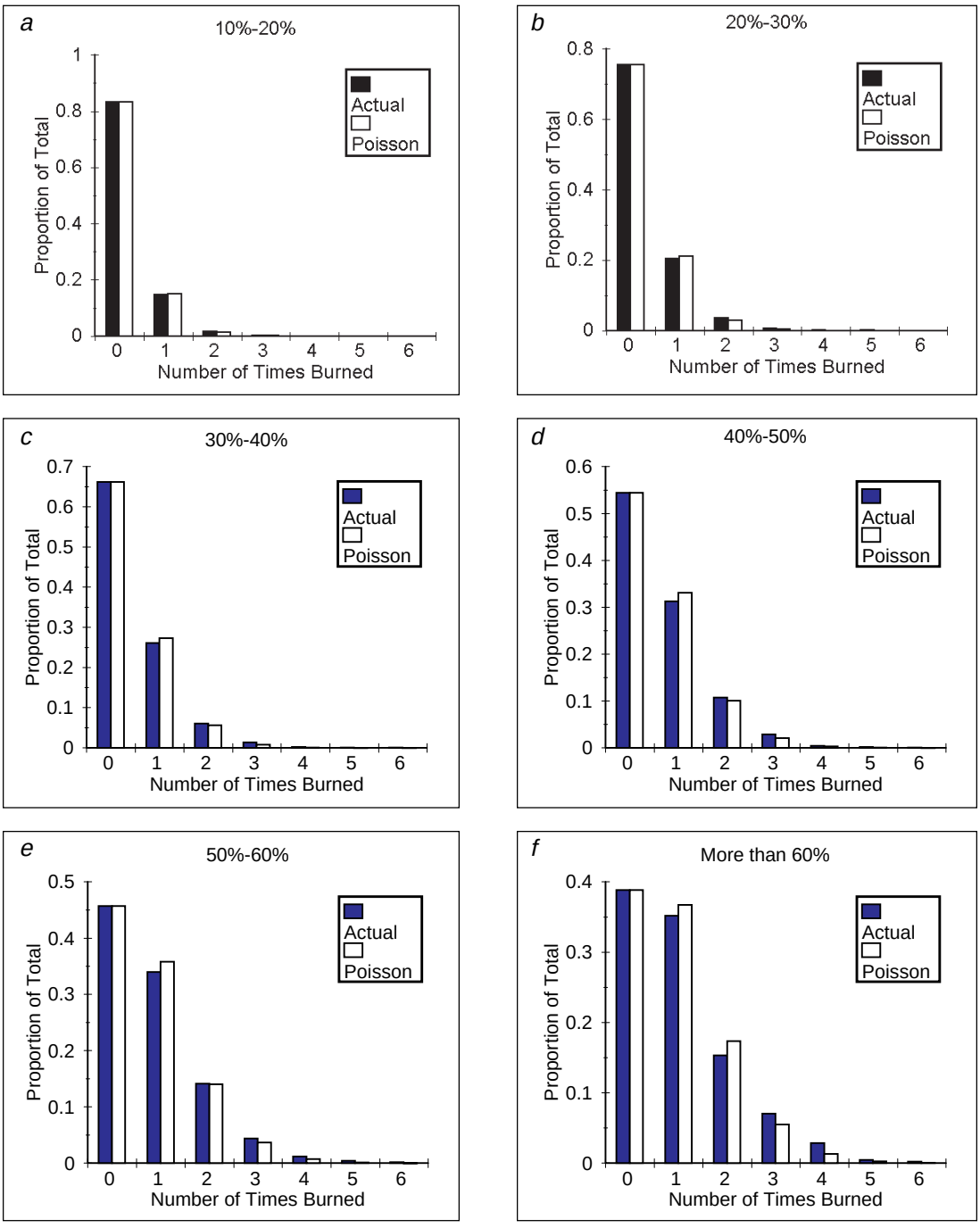

FIGURE 41.17

Reburn patterns for risk decile zones identified through logistic regression (figure 41.13). Poisson expectations for burning 1..*n* times during the time period (1900–1993) are derived directly from fitting the l value to the proportion that did not burn. The "0" bars therefore always match exactly.

TABLE 41.6

Hectares in each fire-risk zone and average fire-rotation intervals based on mapped fires in the twentieth century.

Fire-Risk Class (%)	Area (ha)	Fire-Return Period	
		Actual Frequencies	Poisson Approximation (t / λ)[a]
0–10	1,913,476	2,429.28	2,498.55
10–20	1,440,833	451.21	469.00
20–30	678,572	288.90	303.54
30–40	454,085	194.54	205.81
40–50	295,206	131.92	139.72
50–60	167,508	101.33	108.57
60+	140,791	82.80	89.88

[a] t is the amount of time elapsed, 85 years; λ defines a Poisson distribution (see equation 2, earlier) where in this case k is the number of times a site was burned.

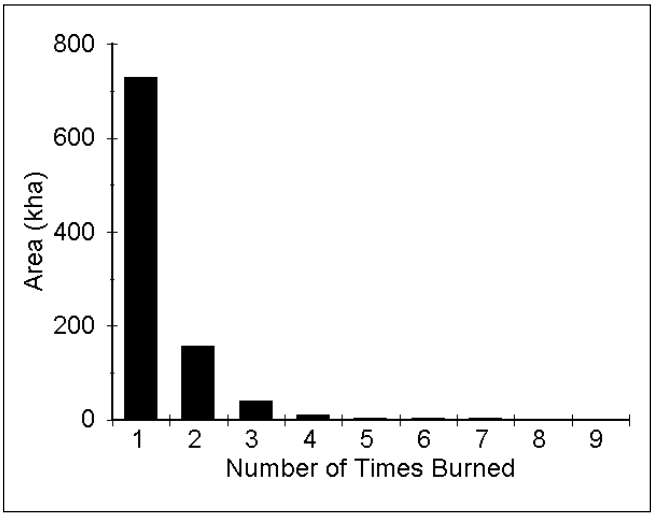

FIGURE 41.18

Reburn patterns for the entire study area.

EVALUATING RELATIONSHIPS BETWEEN FIRE AND WEATHER

The Influence of Drought on Annual Fire Acreage

The overall fire patterns (figures 41.2 and 41.3) suggest that weather may have an influence on acreage burned. In the twenties, and thirties, the late fifties and the eighties—all periods that we would associate with drought—there were increases in fire acreage (figure 41.3). To quantify these relationships we utilized historical weather data (daily precipitation and temperature) from areas near the SNEP study area. The available data set was weather station data compiled by EarthInfo, Inc., of Boulder, Colorado, extending to 1989. Fourteen stations were reasonably close to the Sierra and had daily temperature and moisture data extending back to 1933 (fifty-seven years) (table 41.7; figure 41.19).

To compare these data with annual fire acreage, we averaged the precipitation and temperature data over all of the sites. Because several of the stations are very close geographically, some of them were averaged separately and their average was treated as a single station entry. This was done for Sacramento and Davis, and for Hanford, Orange Cove, and Visalia. Many daily records are missing in this database. For a given station, if more than 10% of the data were missing from the weather record, it was not included in the average for that year or season. To compute yearly or seasonal estimates of rainfall and temperature, we summed daily precipitation and high-temperature readings for each station.

Attempts to correlate fire with annual patterns of precipitation and temperature produced no significant patterns. Because annual precipitation is dominated by winter storms that may not affect fires directly, we repeated the analyses with weather data restricted to the months March through October. Using these data, we found significant relationships between temperature and precipitation (table 41.8). Fire acreage was positively correlated with cumulative seasonal temperature and negatively correlated with seasonal rainfall. To build a simple index comparing both of these understandings, we normalized the values for cumulative temperature and rainfall and created a simple drought index of temperature minus rainfall. We regressed this index on the natural log of fire acreage and obtained a modest positive relationship (figure 41.20).

The relationship was not particularly strong, but yearly fire patterns probably have a strong random component. All of the extreme fire years occurred during years that we would classify as hot and dry, but there were many hot, dry years with very little fire activity (figure 41.21).

TABLE 41.7

Stations used to compute seasonal precipitation, temperature, and drought indices for the Sierra Nevada, 1933–89.

Stations Chosen	Starting Year	Elevation (m)	Annual Rainfall (cm)
Chico University Farm	1906	58	64
Davis Experimental Farm	1917	18	45
Hanford	1927	76	21
Hetch Hetchy	1931	1,180	89
Independence	1927	1,204	13
Modesto	1931	27	31
Nevada City	1931	847	140
Orange Cove	1931	131	32
Red Bluff	1933	103	58
Sacramento	1877	24	47
Sonora	1931	533	80
Susanville	1931	1,265	37
Tahoe City	1931	1,898	81
Visalia	1927	101	26

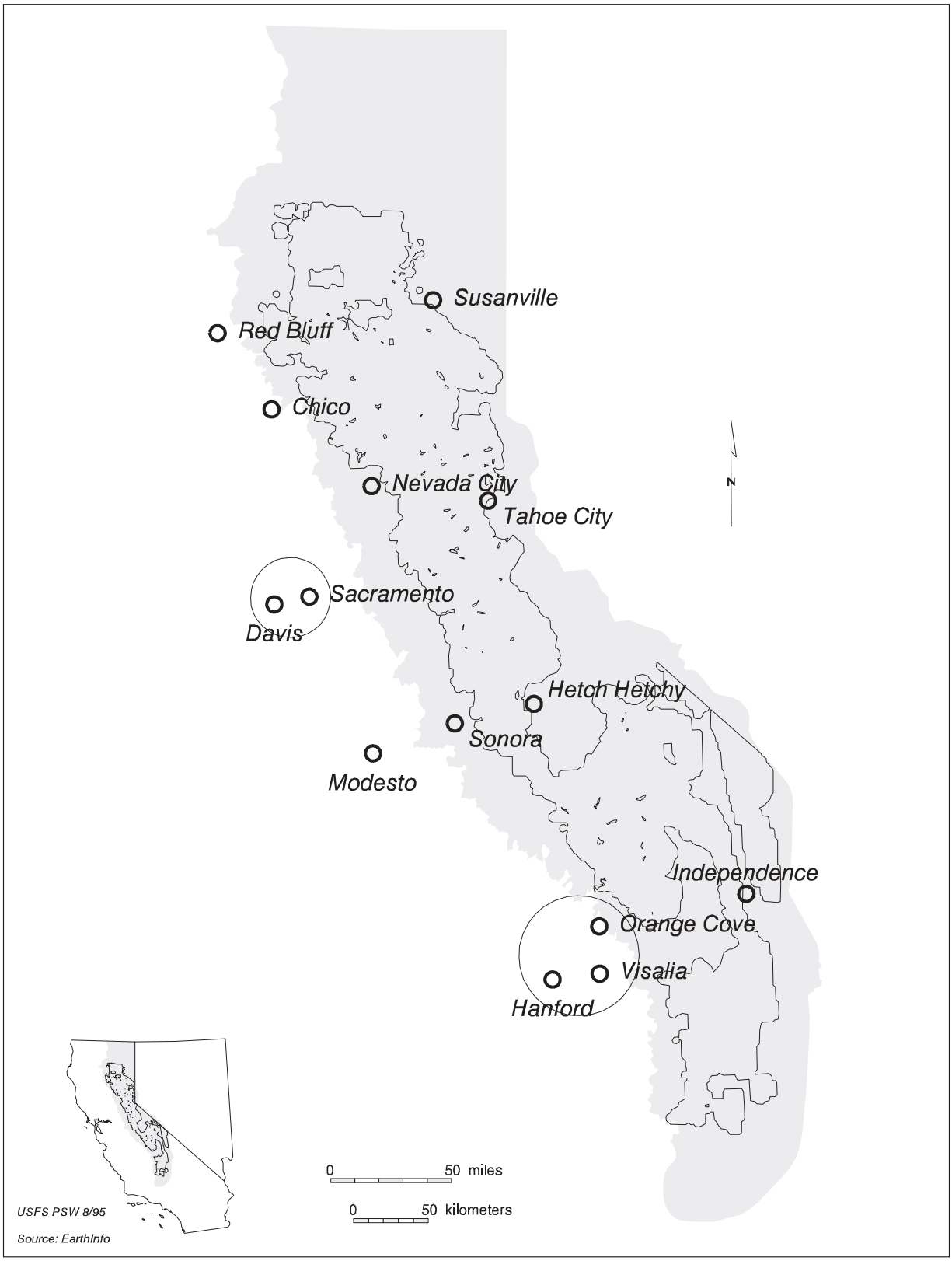

FIGURE 41.19

Locations of fourteen stations for which daily weather data (temperature and precipitation) were available for the period 1933–89. Data from circled stations were averaged and treated as a single station when developing yearly averages.

TABLE 41.8

Correlation between fire and seasonal weather based on fifty-seven years (1933–89) of data collected at fourteen stations. The significance of the correlations is given in parentheses.

	Fire	Rainfall	Temperature
Rainfall	–0.360 (0.006)		
Temperature	0.350 (0.008)	–0.255 (0.056)	
Year	0.042 (0.754)	0.041 (0.759)	–0.126 (0.351)

Spatial and Temporal Patterns of Drought

While longer-term weather data for the Sierra must be inferred from a few valley stations, in the more recent past far more stations have reported, including some higher-elevation sites. For the most recent decade available to us (1979–89), 132 stations in and around the Sierra Nevada reported both temperature and precipitation on a daily basis. In elevation, they ranged from 0 to 2,500 m (0 to 8,250 ft), and while the distribution is not ideal for describing the weather in the Sierra Nevada, a fair number of the stations are in the elevation zone where most of the fires occurred.

Utilizing the Keetch-Byram Drought Intensity Index

From a mechanistic standpoint, fire frequency should be related to the amount of time that a specific area is highly flammable. Each unit of time during which an area is in a highly flammable condition contains some chance that an ignition will occur within that area (fire will either start or spread into that area). If weather is extreme when the ignition occurs, the fire will spread rapidly, likely escape initial containment, be resistant to control, and end up on the map. One potential tool for measuring daily drought is the Keetch-Byram drought intensity index (KBDI) (Keetch and Byram 1968). This index measures deep drying of the litter and is therefore also related to the flammability of live fuels (Keetch and Byram 1968; Burgan 1988). The index ranges from 0 to 800 in value; values greater than 500 are associated with periods of fairly severe drought.

Following this logic, we used the KBDI to measure drought, considering days with KBDI values greater than 500 to be drought days. We then computed the average number of drought days per season for the 132 stations in and around the Sierra Nevada for the period 1979–89. For all stations we started the computations on March 1, with an initial index value of 0.0. Because elevation was the most important determinant of fire frequency, we then regressed these decadal averages on the elevation of each station.

FIGURE 41.20

The natural log of yearly fire acreage regressed on a simple drought index: Σdaily max temp minus Σdaily rainfall, based on the average of fourteen stations, with the units normalized to range between 0 and 1.

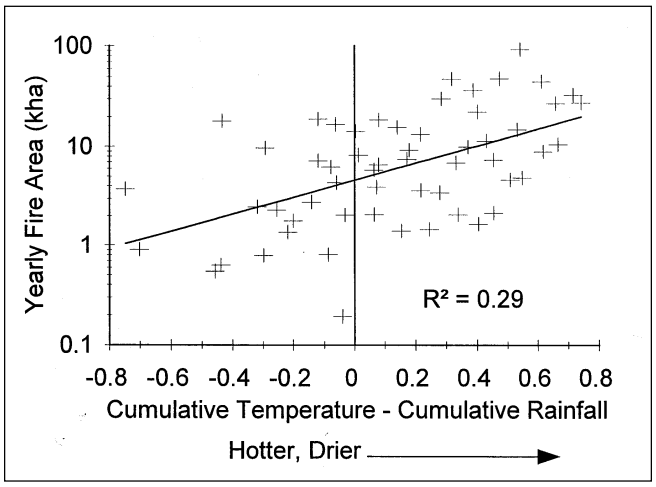

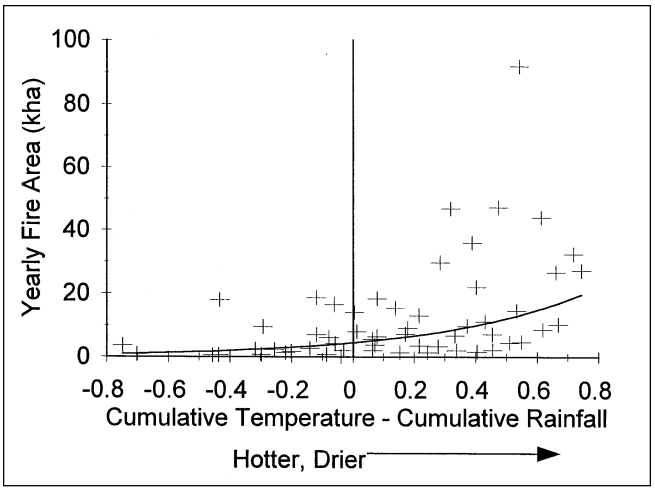

FIGURE 41.21

The regression in figure 41.20, back-transformed and presented on a linear scale. All years with extremely high acreage burned are identified as hot and dry.

Drought As a Function of Elevation

There was a significant negative correlation between elevation and the number of drought days (figure 41.22), with drought levels remaining high (arguably higher) well up into the foothills zone. Because KBDI indices remained very high in the foothills, during drought years some of the highest readings were reported in the zone where there were frequent fires (compare plates 41.5 and 41.6). In order to compare drought days with burn frequencies, we binned the stations into 100 m (3,330 ft) elevation bands and compared the average number of drought days with the fire frequency for those same elevation zones. When the numbers of drought days were scaled to the same maximum value as the burn-frequency data, the patterns were similar (figure 41.23). The elevation at which fire activity

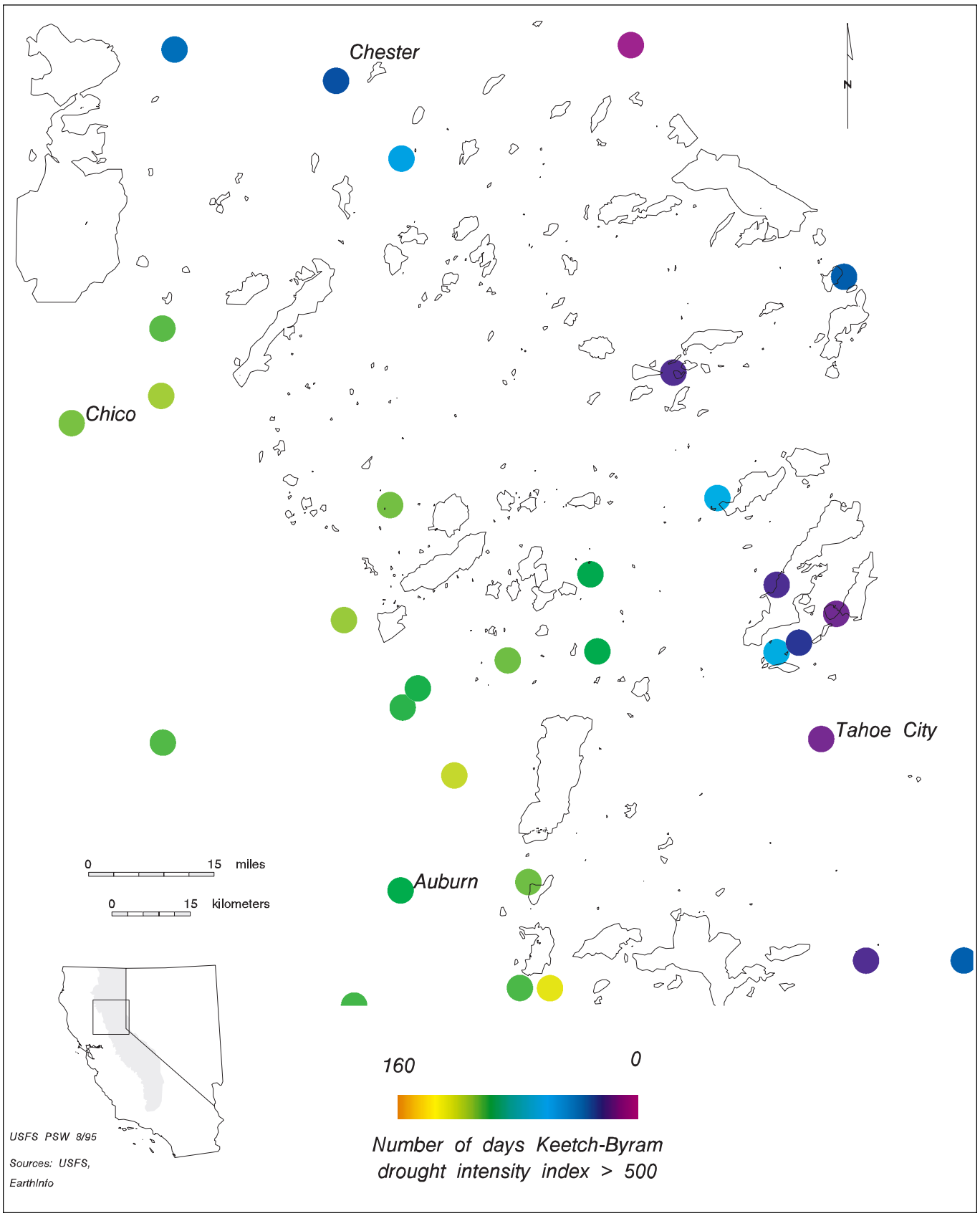

PLATE 41.5

Average number of drought days for the period 1979–89 for an area of the northern Sierra chosen due to the high density of recording stations.

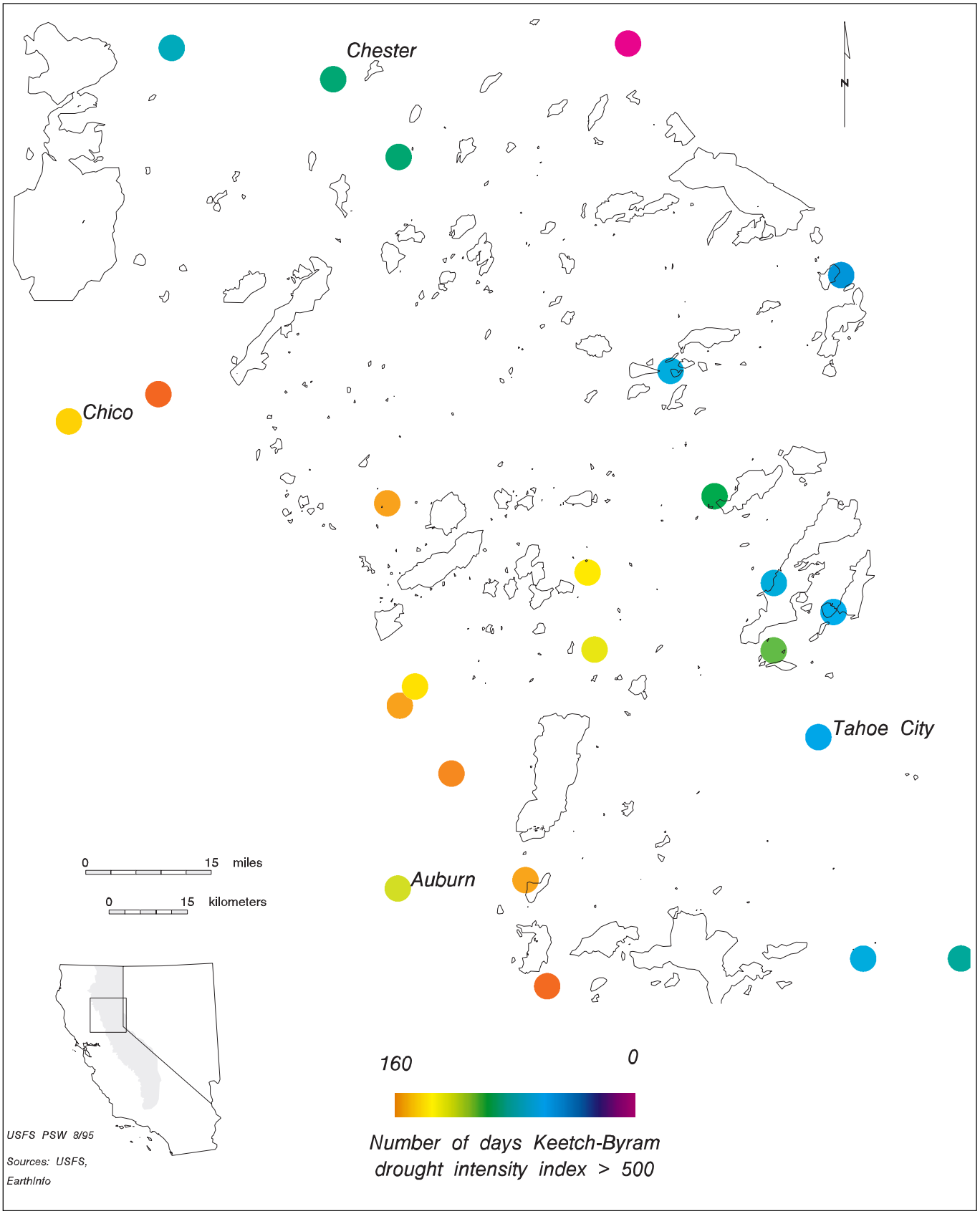

PLATE 41.6

Number of drought days in 1987 for the area shown in plate 41.5. More area burned in 1987 than in any year since the 1920s.

vanished in the Sierra was approximately the same elevation at which there were, on average, no days with KBDI levels greater than 500.

Drought As a Temporal Phenomenon

During the 1980s, there was a wide range in seasonal temperatures and precipitation: 1987 was an extreme fire year, 1982 was one of the least droughty years in the last fifty-seven years, and 1979 was about average. Binning the stations into 100 m elevation groups and comparing these three years reveals parallel patterns, with 1987 having more drought days at all elevations and 1982 having fewer (figure 41.24). When compared to the decade average, stations averaged twenty-two more drought days in 1987 and twenty fewer in 1982. Although the sample was small, at least for the decade of the 1980s, drought in the Sierra Nevada appears to have been highly synchronized. While each station appeared to have had unique weather (hence the scatter observed in figure 41.22), the effect of drought was to increase the number of drought days for all stations. Hence, drought simultaneously enlarged the window of opportunity for extreme fire to occur for all sites and provided a window of opportunity for higher-elevation sites that would normally be too cool and wet.

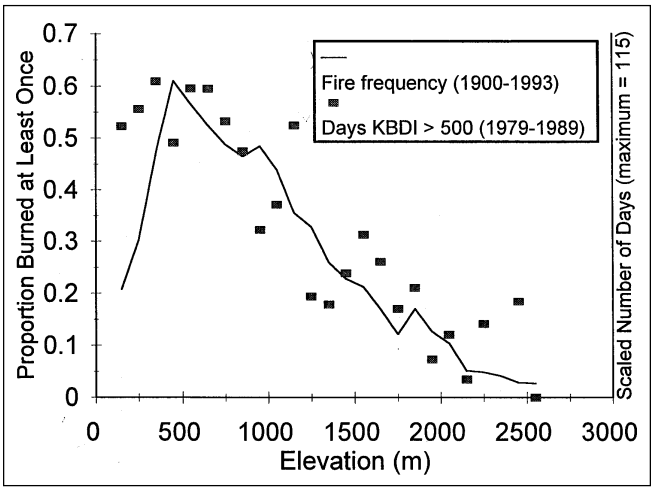

FIGURE 41.23

Average number of drought days for 132 stations (1979–89) grouped into 100 m elevation bins and compared with the fire/frequency pattern based on all mapped fires. The number of drought days has been scaled so that its maximum is 0.61, the maximum fire-frequency level.

SUMMARY

Throughout these analyses, we have assumed that the fire maps developed by the U.S. Forest Service were reasonably accurate and the record reasonably complete. Although we have verified their accuracy for the most recent years (1980–92), we have no direct means to test these assumptions throughout the twentieth century. If there are omissions, they would most likely be concentrated in the smaller fires early in the twentieth century. Most of the results presented in this chapter, however, would be either unaffected or strengthened by these

FIGURE 41.22

Average drought days, defined as days with KBDI levels greater than 500, for the period 1979–89. Each point represents an individual recording station (n = 132). Drought remains high up to about 750 m elevation and then declines. No stations higher than 2,600 m reported weather data during this period.

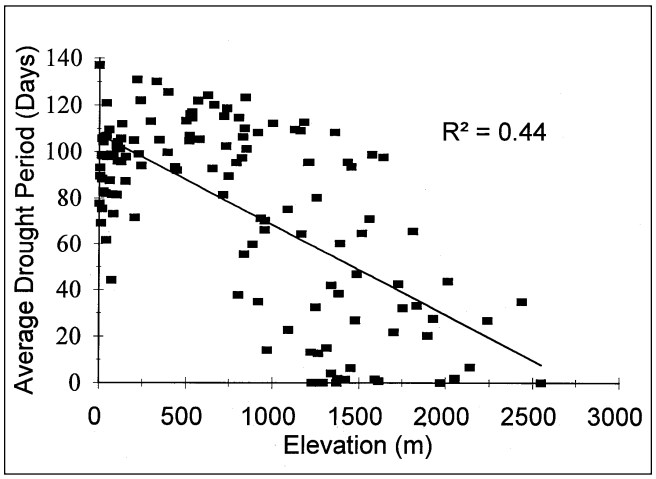

FIGURE 41.24

Average number of days with KBDI values greater that 500 on elevation for the years 1979, 1982, and 1987. Weather station data (approximately 100 stations had complete weather data for each year) was grouped into 100 m elevation bins and averaged.

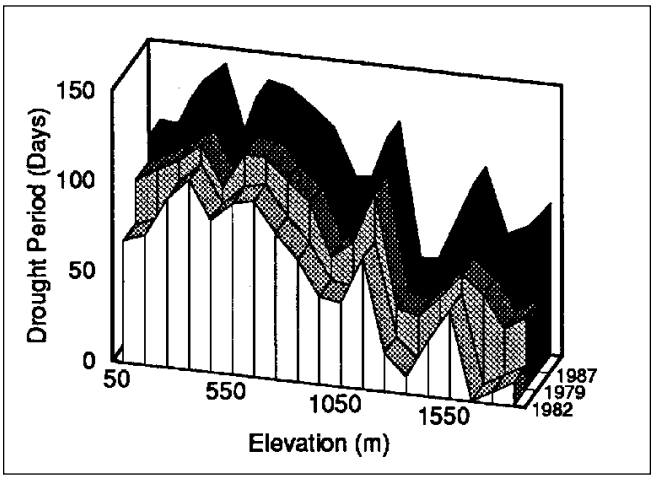

TABLE 41.9

The ten years with the greatest area burned, 1933–89. Rankings are based on fourteen weather stations in the Sierra for the months March through October.

Year	Area Burned (ha)	Proportion Caused by Lightning	Temperature Rank[a]	Rainfall Rank[b]	Cumulative KBDI Rank[c]	Maximum KBDI Rank[d]
1987	91,869	0.98	8	13	11	27
1960	47,204	0.10	13	9	5	1
1942	46,868	0.00	18	38	44	12
1959	43,950	0.09	7	2	7	8
1977	35,841	0.27	19	5	37	37
1936	32,329	0.00	1	18	10	7
1961	29,695	0.04	22	23	17	13
1934	27,172	0.02	2	4	2	17
1939	26,581	0.04	3	30	12	11
1970	21,983	0.00	17	7	6	10

[a]1 is the hottest, 57 the coolest.
[b]1 is the driest, 57 the wettest.
[c]Cumulative KBDI levels summed for each season; 1 is the highest cumulative value, 57 the lowest.
[d]Daily KBDI values are averaged for the fourteen stations, and the highest daily value for each season is recorded. 1 is the highest, 57 the lowest.

potential omissions. Acreage statistics and patterns would be largely unaffected, because the larger fires contribute most of the acreage. In particular, the patterns of fire risk with elevation and overlap would be robust, because these statistics were based on all twentieth-century fires. Some of the time-trend data could be changed if significant early fire acreage was omitted. We might have a slight downward trend in total acreage, and human-caused fires would be down even more dramatically, but acreage in lightning fires would still almost certainly be up. Data on the number of fires per year are probably the most sensitive to the potential omission of small fires (most fires are small), but these patterns remain similar and the inferences unchanged even when small fires are excluded from the analyses (Weatherspoon and Skinner 1996). We therefore believe that analyses based on the mapped fires present a reliable picture of fire patterns in the Sierra Nevada.

Based on these analyses, we feel that the following points have been adequately demonstrated or can reasonably be inferred:

- Fires will occur in the high-risk zones. We feel that the consistency of these patterns is quite remarkable. Consider figures 41.10 and 41.11, which show fire before and after 1940. These patterns are nearly identical, even though the data for the pre-1940s period is heavily weighted by human-caused fires in the 1920s and the data for the post-1940s pattern is weighted by lightning-caused fires in 1987 and 1990. Stand structure, population and land use patterns, and fire-suppression technologies have changed remarkably over this period.
- Within a given risk zone, fire locations will be, for the most part, random. This is really not an unexpected result, given the long fire intervals. Many investigators have found similar patterns when examining systems with long fire-return periods, finding patterns that conform to Poisson expectations (Henstrom and Franklin 1982; Agee 1991) or age structures that fit exponential decline models (Van Wagner 1978, but see Baker 1989; Pitcher 1987; Johnson and Larsen 1991). In addition, these fires all occurred in the context of suppression, and hence probably burned under fairly extreme conditions. Extreme fires are much less sensitive to fuels and topography than are more moderate fires (Turner and Romme 1994).
- If current stand conditions are not altered, current levels of suppression cannot prevent large, stand-replacing fires.
- Periods of drought of the magnitude that has occurred several times in the twentieth century will cause a significant increase in the likelihood of extreme fire events and will likely be accompanied by large wildfires.
- The last drought, though not the most extreme in terms of weather, caused the most extreme fire behavior. Several recent large fires have been caused by lightning, which is also unusual. The degree to which these years are unusual can be seen by examining the "worst" fire years on record (table 41.9). In general, while lightning has frequently accounted for as much as 40% of the fire acreage, it has not been a factor in the extreme fire years. Lightning accounted for less than 10% of the acreage in seven of the ten worst fire years (table 41.9). In 1987, however, lightning accounted for 98% of the acreage. Based on seasonal weather statistics, there was no reason to expect fire behavior in 1987 to be unusual: 1987 was not the worst drought year, nor were the 1980s the period of worst drought. Certainly 1934, 1959, and 1960 were hotter, drier, and droughtier than 1987, and the period 1933–40 was hotter and drier than the late 1980s (table 41.9).

It is difficult to determine the extent to which these recent fires should impact our understanding of the system. It is, of course, possible that these fires simply represent very unusual

weather. It should be noted that the late 1980s saw many extreme fires across the western United States, including the 1988 Yellowstone fires. While fuel buildups may be implicated in these events, patterns of fuel accumulation and the impacts of fire suppression in other locations may have little to do with the condition of the lower-elevation Sierra Nevada. Fire patterns in the Greater Yellowstone Ecosystem, for instance, appear to be following very long natural cycles (Romme 1982; Romme and Despain 1989).

There are, however, subtle signs that the situation in the forest may well have changed. These signs are found in the decoupling of human-caused and lightning-caused fire patterns. Human-caused fires have been declining steadily—in total acreage, in number, and in average size. This pattern is probably due to a combination of increased efficiency in fire suppression and public education. Lightning fires have remained constant or have increased over this same time period, and this statement was true prior to the 1987 fires.

Lightning fires are grouped both in space and time. Because of this grouping, the resources required to suppress each ignition become critical. If changes in forest structure and fuel loading are increasing the suppression fire costs per acre, then it will take fewer simultaneous ignitions to exhaust the local resources.

While there are unknowns concerning recent extreme fire behavior, we believe that, taken as a whole, these points reasonably lead to the following conclusions concerning land-management policies:

- We can accurately describe risk zones in the Sierra; hence we can approach fire control efficiently. In the twentieth century 50% of the fire acreage has been below 1,300 m, and 92% has been below 2,000 m (figure 41.25). Fire control policies must recognize this reality.
- If conditions present in the twentieth century (fuels, weather, and suppression capabilities) continue, we can expect the patterns developed in these analyses to be stable into the near future. Absolute acreage will go up and down with shifts in weather, but fires will be probably be concentrated in the higher-risk (lower-elevation) zones.
- The high frequency of fire in lower-elevation areas, coupled with a high degree of randomness, suggests a zonal strategy. The goal must be to reduce the probability of destructive fires within these areas, either by increasing suppression capabilities to the extent that few fires escape initial containment (assuming that this is possible) or by reducing fuels to the point that canopy trees and structures are not threatened by fires when they occur.
- Either increasing suppression efforts or reducing fuels sufficiently to have a significant impact on fire behavior will be extremely costly. It is essential to evolve control plans that are cost-effective on a per-acre basis and that have a strong strategic emphasis so as to efficiently treat the most critical areas. The acreage distribution of the risk categories, which shows relatively small acreages in the highest risk categories (table 41.6; figure 41.13), suggests that strategies that concentrate treatment in high-risk zones may be cost-effective.
- Because within a risk zone overlap patterns of fire are largely random, we believe that fire-risk management would be best served by a policy that first allocated resources to control the destructive effects of fire in high-risk topographic zones. Within these zones, suballocations would appropriately be based on many factors, such as the consequences of fire and the costs of either treatment or suppression. We believe that in this suballocation process it would be prudent also to consider the number of times that the site has burned in the past as a risk factor. We do not believe, however, that localized history of burning should dominate resource allocation decisions.

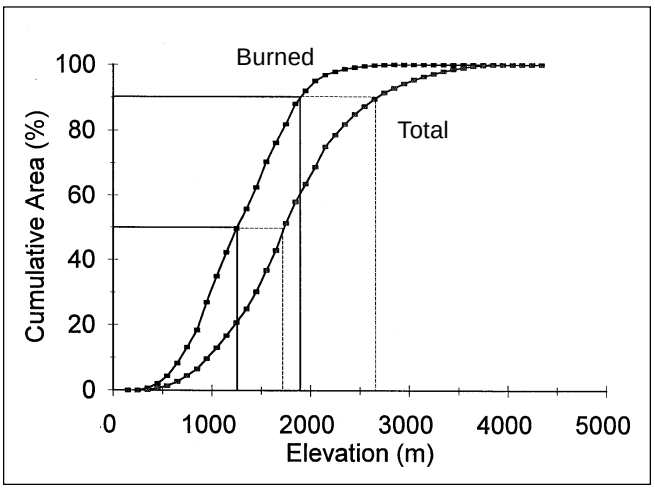

FIGURE 41.25

Fire area and total land in the study area. Lines mark the 50th and 90th percentiles for both distributions.

ACKNOWLEDGMENTS

We would like to acknowledge Carl N. Skinner for providing analyses demonstrating the divergence between human- and lightning-caused fires in the Sierra. In addition, we would like to acknowledge the national forest employees past and present who created the fire maps, without which none of these analyses could have been accomplished; the CALOWL EIS team; the SNEP GIS team, and the members of the SNEP disturbance subgroup. In addition we would like to thank two anonymous reviewers for their suggestions, as well as many others who provided additional reviews and comments. This study was supported (in part) by the Sierra Nevada Ecosystem Project as

authorized by Congress (HR 5503) through a cost-reimbursable agreement No. PSW-93-001-CRA between the U.S. Forest Service, Pacific Southwest Research Station, and the Regents of the University of California, Wildland Resources Center.

REFERENCES

Agee, J. K. 1991. Fire history along an ecological gradient in the Siskiyou Mountains, Oregon. *Northwest Science* 65:188–99.

——. 1993. *Fire ecology of Pacific Northwest forests*. Washington, DC: Island Press.

Agee, J. K., M. Finney, and R. Gouvenain. 1990. Forest fire history of Desplation Peak, Washington. *Canadian Journal of Forest Research* 20:350–56.

Baker, W. L. 1989. Effect of scale and spatial heterogeneity on fire interval distributions. *Canadian Journal of Forest Research* 19: 700–706.

Brown, D. G., and T. J. Bara. 1994. Recognition and reduction of systematic error in elevation and derivative surfaces from 7 1/2-minute DEMs. *Photogrammetric Engineering and Remote Sensing* 60:189–94.

Burgan, R. E. 1988. *Revisions to the 1978 national fire-danger rating system*. Ashville, NC: U.S. Forest Service, Southeastern Forest Experiment Station.

Campbell, G. S. 1977. *An introduction to environmental biophysics*. New York: Springer-Verlag.

Chou, Y. H., R. A. Minnich, and R. A. Chase. 1993. Mapping probability of fire occurrence in San Jacinto Mountains, California, USA. *Environmental Management* 17:129–40.

Chou, Y. H., R. A. Minnich, L. A. Salazar, J. D. Power, and R. J. Dezzani. 1990. Spatial autocorrelation of wildfire distribution in the Idyllwild Quadrange, San Jacinto Mountain, California. *Photogrammetric Engineering and Remote Sensing* 56:1507–13.

Erman, D. C., and R. Jones. 1996. Fire frequency analysis of Sierra forests. In *Sierra Nevada Ecosystem Project: Final report to Congress*, vol. II, chap. 42. Davis: University of California, Centers for Water and Wildland Resources.

Feller, W. 1968. *An introduction to probability theory and its applications*. New York: John Wiley and Sons.

Henstrom, M. A., and J. F. Franklin. 1982. Fire and other disturbances in the forests in Mount Rainier National Park. *Quaternary Research* 18:32–51.

Horn, H. 1971. *The adaptive geometry of trees*. Monographs in Population Biology, no. 3. Princeton, NJ: Princeton University Press.

Hosmer, D. W., and S. Lemeshow. 1989. *Applied logistic regression*. New York: John Wiley and Sons.

Johnson, E. A., and C. P. S. Larsen. 1991. Climatically induced change in fire frequency in the southern Canadian Rockies. *Ecology* 72: 194–201.

Keetch, J. J., and G. M. Byram. 1968. *A drought index for forest fire control*. Research Paper, SE-38. Asheville, NC: U.S. Forest Service, Southeast Forest Experiment Station.

Matyas, W. J., and I. Parker. 1979. *CALVEG: Mosaic of the existing vegetation of California*. San Francisco: U.S. Forest Service, Regional Ecology Group.

Minnich, R. A. 1983. Fire mosaics in southern California and northern Baja California. *Science* 219:1287–94.

Pitcher, D. C. 1987. Fire history and age structure in red fir forests of Sequoia National Park, California. *Canadian Journal of Forest Research* 17:582–87.

Rantz, S. E. 1969. *Mean annual precipitation in the California region*. Menlo Park, CA: U.S. Geological Survey.

Romme, W. H. 1982. Fire and landscape diversity in subalpine forests of Yellowstone National Park. *Ecological Monographs* 52:199–221.

Romme, W. H., and D. G. Despain. 1989. Historical perspective on the Yellowstone fires of 1988. *Bioscience* 39:695–99.

Show, S. B., and E. I. Kotok. 1923. *Forest fires in California, 1911–1920: An analytical study*. Department Circular 243. Washington, DC: U.S. Department of Agriculture.

Strauss, D., L. Bednar, and R. Mees. 1989. Do one percent of forest fires cause ninety-nine percent of the damage? *Forest Science* 35:319–28.

Turner, M. G., and W. H. Romme. 1994. Landscape dynamics in crown fire ecosystems. *Landscape Ecology* 9:59–77.

U.S. Forest Service (USFS). 1996. *Final environmental impact statement: Managing California spotted owl habitat in the Sierra Nevada National Forests of California—An ecosystem approach (CALOWL EIS)*. 2 vols. Berkeley, CA: U.S. Forest Service, Pacific Southwest Research Station.

Van Wagner, C. E. 1978. Age class distribution and the forest fire cycle. *Canadian Journal of Forest Research* 8:220–27.

Weatherspoon, C. P., and C. N. Skinner. 1996. Landscape-level strategies for forest fuel management. In *Sierra Nevada Ecosystem Project: Final report to Congress*, vol. II, chap. 56. Davis: University of California, Centers for Water and Wildland Resources.

Wonnacott, T. H., and R. J. Wonnacott. 1977. *Introductory Statistics*. New York: John Wiley and Sons.